General Disclaimer

One or more of the Following Statements may affect this Document

- This document has been reproduced from the best copy furnished by the organizational source. It is being released in the interest of making available as much information as possible.

- This document may contain data, which exceeds the sheet parameters. It was furnished in this condition by the organizational source and is the best copy available.

- This document may contain tone-on-tone or color graphs, charts and/or pictures, which have been reproduced in black and white.

- This document is paginated as submitted by the original source.

- Portions of this document are not fully legible due to the historical nature of some of the material. However, it is the best reproduction available from the original submission.

COLLEGE OF ENGINEERING

Sincerely yours,

Edmund G. Henneke

Edmund G. Henneke
Associate Professor

VIRGINIA POLYTECHNIC INSTITUTE AND STATE UNIVERSITY

BLACKSBURG, VIRGINIA

VPI-E-77-22 September, 1977

SIGNATURE ANALYSIS OF ACOUSTIC EMISSION FROM GRAPHITE/EPOXY COMPOSITES

Samuel S. Russell[1]
Edmund G. Henneke[2]

Department of Engineering Science and Mechanics

Interim Report
NASA Grant NSG 1238

Prepared for: Materials Application Branch
National Aeronautics and Space Administration
Langley Research Center
Hampton, VA. 23665

[1]Graduate Student
[2]Associate Professor

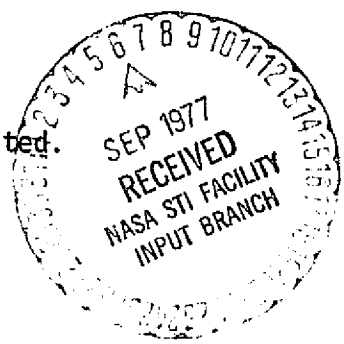

BIBLIOGRAPHIC DATA SHEET	1. Report No. VPI-E-77-22	2.	3. Recipient's Accession No.
4. Title and Subtitle SIGNATURE ANALYSIS OF ACOUSTIC EMISSION FROM GRAPHITE/EPOXY COMPOSITES			5. Report Date September, 1977 6.
7. Author(s) Samuel S. Russell and Edmund G. Henneke, II			8. Performing Organization Rept. No. VPI-E-77-22
9. Performing Organization Name and Address Virginia Polytechnic Institute and State University Department of Engineering Science and Mechanics Blacksburg, Virginia 24061			10. Project/Task/Work Unit No. 11. Contract/Grant No. NASA NSG 1238
12. Sponsoring Organization Name and Address National Aeronautics and Space Administration Langley Research Center Hampton, Virginia 23665			13. Type of Report & Period Covered 14.
15. Supplementary Notes			
16. Abstracts see page ii			
17. Key Words and Document Analysis. 17a. Descriptors composites, acoustic emissions, signature analysis, failure modes, graphite-epoxy			
17b. Identifiers/Open-Ended Terms			
17c. COSATI Field/Group			
18. Availability Statement Distribution unlimited		19. Security Class (This Report) UNCLASSIFIED 20. Security Class (This Page UNCLASSIFIED	21. No. of Pages 22. Price

FOREWARD

This report documents work accomplished under NASA Grant NSG 1238 during the period January, 1976 through June, 1977. The authors wish to express thanks to Ms. Frances Carter for typing the manuscript.

SIGNATURE ANALYSIS OF ACOUSTIC EMISSION FROM GRAPHITE/EPOXY COMPOSITES

ABSTRACT

Acoustic emissions have been monitored for crack extension across and parallel to the fibers in a single ply and multi-ply laminates of graphite/epoxy composites. Spectrum analysis was performed on the transient signal to ascertain if the fracture mode could be characterized by a particular spectral pattern. The specimens were loaded to failure quasi-statically in a tensile machine. Visual observations were made via either an optical microscope or a television camera. The results indicate that several types of characteristics in the time and frequency domain correspond to different types of failure.

TABLE OF CONTENTS

LIST OF ILLUSTRATIONS

LIST OF SYMBOLS

x	an arbitrary function in time domain
X	a complex function in the frequency domain
w	angular frequency
t	a time variable
f	a forcing function in the time domain
F	the fourier transform of a forcing function
H	the natrual frequency response of a system
y	an arbitrary function
T	a time variable
h	a function in the time domain
P	a function in the frequency domain
A	amplitude of a function

1. INTRODUCTION

Acoustic emission is a valuable tool for investigating and predicting fracture of materials. Using techniques that monitor either acoustic energy, energy per unit time or counts of energy over a certain level per unit time, impending fracture has been reliably predicted [1, 2, and 3]. Crack growth has been monitored in structures of such national importance as the Liberty Bell [4].

Relatively little effort has been expended in investigating fracture processes by fourier analysis or similar transforms of the acoustic emission. The basic technique of spectrum analysis of acoustic emissions involves subjecting a sample of material to a mechanical or thermal load and converting by a microphone, transducer or strain gage the acoustic energy released by the material to an electrical signal. The signal is either recorded on a tape recorder for later analysis or is fed directly into a real time transform device. The product of the analysis is a graph of the amplitude versus frequency.

G. Curtis [5] showed a change in the spectrum of acoustic emissions of an adhesive lap joint just prior to failure. A special wide band transducer was built by Curtis for his work. The distortion effects of specimen size and geometry and transducer natural resonances on the response spectrum were discussed.

Graham and Alers [6] found two distinct types of spectra being emitted from steel samples. They concluded that the two spectra types correspond to plastic deformation and crack growth. In reference 7,

Graham and Alers used a video tape recorder to record the emissions from various metals and ceramics for later analysis. The video recorder had the advantage that a portion of the tape can be examined continuously with the tape drive off.

A spectrum analysis was performed by Fleishman [8] on a low carbon steel using an experimentally derived system transfer function to correct for the system geometry and transducer distortion. The transfer function was obtained by using a generating transducer with a known transfer function. The results emphasized the importance of the system's natural response to obtain the spectrum due to the micromechanical activity responsible for the emission.

K. Ono and J. Ucisik [9] took count rate and performed spectral analysis on acoustic emissions from several aluminum alloys. Three different transducers were compared. One of the transducers used was the same type as used in this study, FAC-500 Acoustic Emission Technology Corporation, broad-band transducer. Several different classes of spectra were observed but could not be correlated to a particular micromechanical event.

That fiber reinforced composites have unique acoustic emissions associated with fiber breakage or matrix cracking seems reasonable. These failure processes each release energy and relieve stress in different directions. Matrix cracking should cause a vibratory motion perpendicular to the fiber when a crack initiates parallel to the fiber direction. A fiber breaking should cause a longitudinal vibration and should, because of the nature of the material, be the more energetic

event. The difference in vibratory modes mean corresponding the transfer function would be drastically different for the different failure modes, causing even greater differences in the spectra of a fiber break or a longitudinal crack.

Despite expected differences little useable work has been done relating a characteristic spectra to a particular failure mode in a fiber reinforced composite. Speake and Curtis [11] experimented with carbon fiber composite specimen size and geometry. Their results showed a strong dependence of the spectrum of an acoustic emission upon specimen and mounting jig geometries. However, they were able to find some characteristic frequencies of emissions from different types of fibers.

A comparison between the spectrum of acoustic emissions recorded from Boron/Aluminum and Boron/epoxy with a semiconductor strain gage and an accelerometer was performed by Mehan and Sturgeon [12]. Mullin and Mehan [13] reported different frequency characteristics for different failure modes in low volume fraction Boron epoxy samples. However, their work is incomplete as no direct correlation between a failure mode and a certain spectrum was given.

Henneke and Herring [14] recorded emissions from Boron/Aluminum composite specimens with a condenser microphone. Some of the advantages were that the microphone was broad-band and that the microphone did not touch the specimen, and hence did not alter the vibration modes of the specimen. The spectra acquired displayed families of characteristics, but some of the spectra were irregular. Some of the specimens were tested up to a load less than ultimate and then etched until the matrix

was removed. The number of fiber breaks was approximately the same as the number of emissions occuring during the test. The spectrum of emissions were compared with the spectrum of an object hitting the specimen and with the spectrum of an end tab breaking away from a specimen. The spectrum of the emissions were mostly high frequencies while the tab pop and the impact spectrum were composed mainly of low frequencies. However, the differences in the acoustic emission spectra rule out any simple correlation between a family of spectra and a particular failure mode.

A characteristic spectrum for each failure mode could yield valuable information to a designer. A designer could evaluate the inservice advanced composite structure and know the causes of weakness in the structure. He could then redesign to prevent a certain type of failure. The objective of this study was to ascertain if characteristic frequencies exist for various failure modes in advanced composite materials. In this study all tests were performed on graphite/epoxy specimens.

2. FOURIER ANALYSIS AND ITS USE IN VIBRATION ANALYSIS

Fourier analysis can be thought of as a transform that yields the relative amplitudes of an infinite number of waves that compose the signal being analyzed. A fourier transform can simplify results and lead to a solution in some problems. In most cases a simplification in the frequency domain results and an inverse transform leads to a solution. However, the technique is used here to yield a frequency domain representation of a transient signal which is examined for pecularities of properties unique to a family of signals.

In this section the relevance of fourier analysis to the study of vibrations is duscussed. Truncation and discretization are introduced into the analysis and the results and implications are considered. The fast fourier transform is shown to be an effective means of computing the discrete spectra of a function.

The continuous fourier transform pair is usually introduced as [15]

$$X(w) = \int_{-\infty}^{\infty} x(t)e^{-iwt}dt \qquad (1)$$

$$x(t) = \int_{-\infty}^{\infty} X(w)e^{iwt}dw \qquad (2)$$

where $x(t)$ is time domain function, $X(w)$ is the frequency domain representation and t and w are continuous variables.

The importance of the fourier transform in vibration theory lies in its ability to yield a solution to a complicated vibration problem using the system characteristic solution and the applied load or forcing

function. For a general vibration system the fourier transform of the response x(t) to a forcing function f(t) is

$$X(w) = F(w)H(w) \tag{3}$$

where F(w) is the fourier transform of f(t) and H(w) is the natural frequency response or transfer function [15]. If the natural response of the system is known or is flat, the frequency components of the forcing function can be found by multiplying X(w) by the inverse of the natural frequency response.

Structural damping plays an important role in determining the characteristics of the natural frequency response of a system. As damping increases, the frequency response curve of vibratory systems tends to flatten and broaden, with the peaks becoming less influential. In systems with little damping the fundamental frequency and its harmonics become dominant. A system with no damping can vibrate only at the natural frequency and its harmonics [16].

For fourier analysis of most experimental data, the definitions given in equations (1) and (2) can not be used. Experimental data is obtained in a form that is finite in duration and usually discretized. It is necessary then to alter equations (1) and (2) to handle real data in this form. In transforming the continuous fourier transform pair to the discrete transform pair an abbreviated version of a procedure used by E. O. Brigham [17] will be summarized. First the convolution theorem will be presented, then the effects of convolution on the discretization and truncation processes needed to implement a fourier analysis on a

digital computer will be discussed.

The convolution integral is defined as [17]

$$y(t) = \int_{-\infty}^{\infty} x(T)h(t-T)dT \tag{4}$$

Here, $y(t)$ is called the convolution of $x(t)$ and $h(t)$. The operation of convolution is commutative, that is

$$y(t) = \int_{-\infty}^{\infty} x(T)h(t-T)dT = \int_{-\infty}^{\infty} h(T)x(t-T)dT \tag{5}$$

The significance of the convolution integral can best be realized through use of a graphical technique for evaluating the convolution integral. The following steps summarize the graphical technique: [17]

1. Take the mirror image of $h(T)$ about the vertical axis; i.e., flip the function $h(T)$ about the vertical axis.
2. Slide $h(-T)$ down the time axis an amount t.
3. Multiply the flipped and displaced function of $h(t-T)$ by $x(T)$.
4. Find the area of the product of the flipped and displaced function of $h(t-T)$ and $x(T)$.

The four steps above result in one point on a continuous curve for continuous functions $h(t)$ and $x(t)$. To find an approximation to the total convolution curve steps 2,3, and 4 should be repeated at selected intervals of t to give a number of points along the curve. The results of the convolution integral can be thought of as a smearing together of two functions.

The importance of convolution to fourier analysis is a result of the convolution theorem. The convolution theorem states that multipli-

cation of any two functions in one domain (time or frequency) results in convolution of the two functions in the transformed domain (frequency or time). As an example, if two functions of time were multiplied together then the transform of the product equals the convolution in the frequency domain of the two functions after each has been operated on by the fourier transform.

In order to use the fourier transform on any real data the integral must be discretized by multiplying the function being transformed by a series of equally spaced impulse functions. Also the function being transformed must be truncated by multiplying by a square pulse whose length is determined by the instruments used to capture the transient emission. The transient recorder used in these experiments had the ability to store 2048 equally spaced points to discretize the signal. The length of the signal recorded was 2047 times the discretization interval. Because of the convolution theorem the fourier transforms of both the infinite series of impulse functions and the square pulse are convoluted with the true fourier transform of the signal in the frequency domain.

The fourier transform of an infinite series of impulse functions equally spaced a distance T apart is another series of infinite impulse functions with a frequency spacing of 1/T. As a consequence of the convolution theorem, the portion of the fourier transformed signal with a higher frequency than 1/2T will be folded over a line at 1/2T on the frequency axis and added to the lower frequency spectrum. This is the Nyquist phenomenon, and 1/2T is called the Nyquist frequency. In

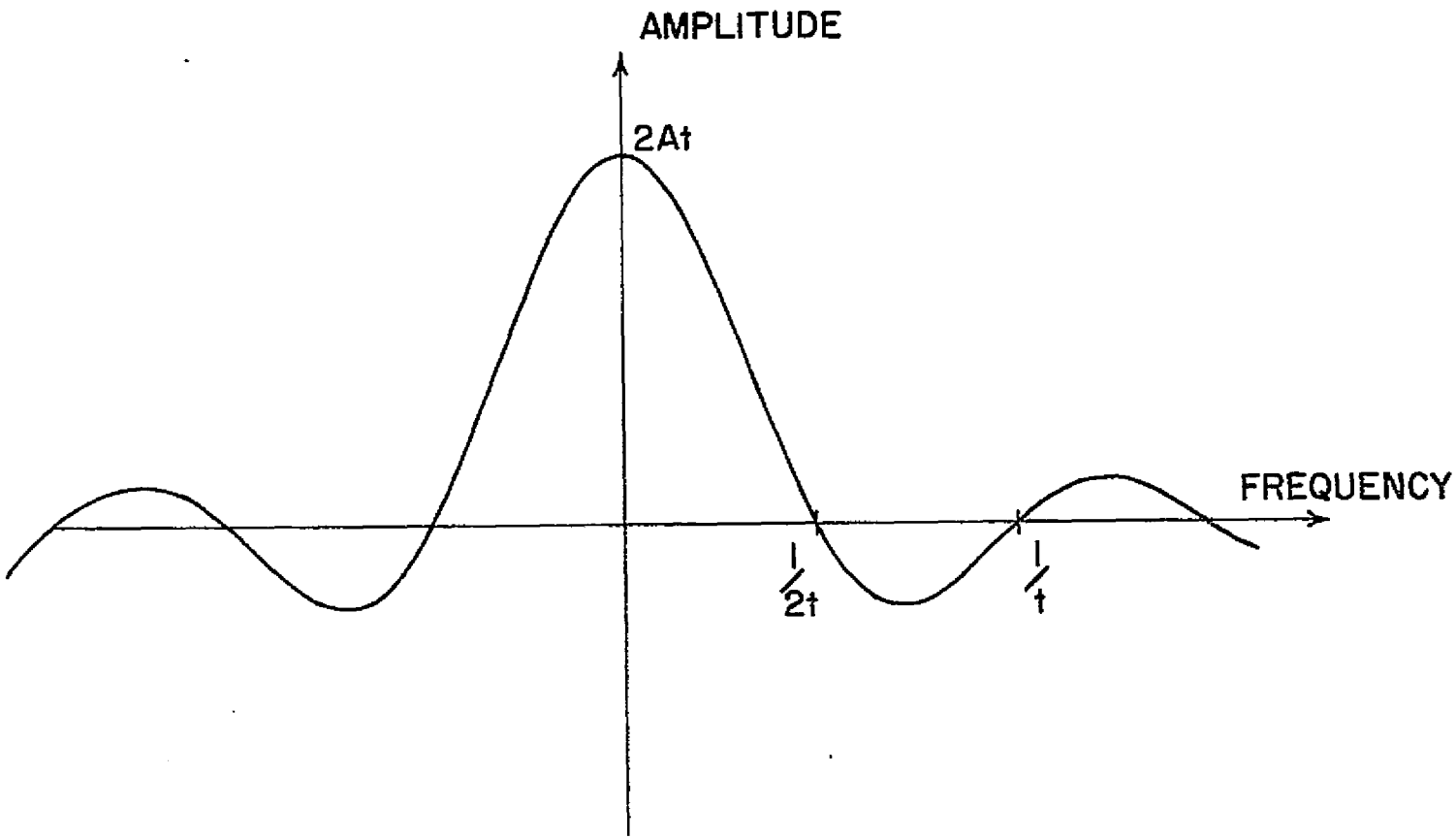

Figure 1. Fourier Transform of Square Pulse of Amplitude A and Duration t

practice the Nyquist ghost frequencies can be eliminated by using electronic filters to cut out any frequency components above the Nyquist frequency.

Because of equipment and computational limitations, the number of points selected to represent a signal is finite. Simple truncation of a signal is equivalent to multiplication of a signal by a square pulse. In the frequency domain this is equivalent to convolution of the fourier transformed signal with the fourier transformed square pulse. The fourier transform of a square pulse of length and height A is the so called sink function or

$$P(f) = 2At \frac{\sin(2\pi tf)}{2\pi tf} \qquad (6)$$

A graph of equation (5) is shown in Figure (1). Convolution of equation (5) and the true fourier transformed signal causes error by smoothing or blurring part of the signal and introducing false peaks in other parts of the spectrum. The problems associated with truncation of the time signal are called leakage.

One of the most common means of reducing leakage effects is to choose the frequency discretization step to be 1/t. When the discretization step is chosen to be 1/t the impulse functions not centered with the sink function are multiplied by zeros and convolution error is reduced. Thus when the sink function is convoluted with the discretized transformed signal the result is no or little smoothing.

A problem with transient signals is that the length of the signal is not known, or the signal may appear to be multiplied by a triangular

pulse. These characteristics cause leakage even through the frequency interval was chosen, as described previously, to be the inverse of the length of the square pulse. If another function, for example, a truncated cosine or sink function is used to truncate or window the signal, the leakage is reduced since the side lobes of the transformed function are smaller in amplitude than for the sink function.

The Fast Fourier transform is a recently developed technique [17] that provides a very efficient means of calculating the discrete fourier transform. The Fast Fourier algorithm reorders the sequence of numbers and takes advantage of similarities and symmetries of the complex exponential function.

For direct implementation of a discrete Fourier transform on a high speed computer the computation time is proportional to N^2, where N is the number of sinusoids or frequency points calculated. For the Fast Fourier Method the computation time is proportional to $N \log_2 N$ [17]. Obviously for most data series this means a great savings in computer costs.

The Fast Fourier algorithm used in this analysis was published by Cooley, Lewis and Welch [18] in 1969 as a subroutine. The main program reads the input data and orders it so that it can be operated upon by the FFT subroutine. A separate subroutine is used to interpret and graph the output of the FFT subroutine. The truncation window used is a zero centered displaced cosine function. Several windows were used but the displaced cosine is one of the best for reducing leakage. This window emphasizes the initial portion of the signal and is therefore

ideal for transient analysis. A listing and brief discussion of the program is included in the appendix.

3. EXPERIMENTAL PROGRAM

The specimens (discussed later) were subjected to quasi-static tension load on an Instron Model 1125 test machine at a crosshead rate of .01 to .05 in/min, depending on the test. An optical microscope mounted on a stage attached to the crosshead, and later a television camera with a close-focus lens, was used to observe the growth of a crack from a damaged region. The transducers used to monitor the acoustic emissions were a Panametrics 5070AE-0.1CC cross-coupled, 1/4" x 1/4" unhoused transducer and an Acoustic Emission Technology, model FAC 500 housed transducer, 1" diameter. Both the transducers were bonded to the specimen with double sided sticky tape and held in place by masking tape.

The signal was transmitted from the transducer to a Panametrics ultrasonic preamplifier, then to a Tektronix type 1A7A differential amplifier, and was recorded on a Honeywell 5600B tape recorder at 60ips. The dynamic response and amplification of the electrical equipment is discussed below. The settings of 40 dB on the preamplifier and .2 Volts/cm on the Type 1A7A differential amplifier were experimentally determined to be best suited to keep the signal significantly large in amplitude without saturating the tape recorder amplifier. The band width selector on the differential amplifier was set to pass frequencies between 100 Hz and 300 KHz. This setting reduced low frequency noise and insured no Nyquist-related problems existed. On a parallel track on the tape recorder, voice comments on the test were recorded. An

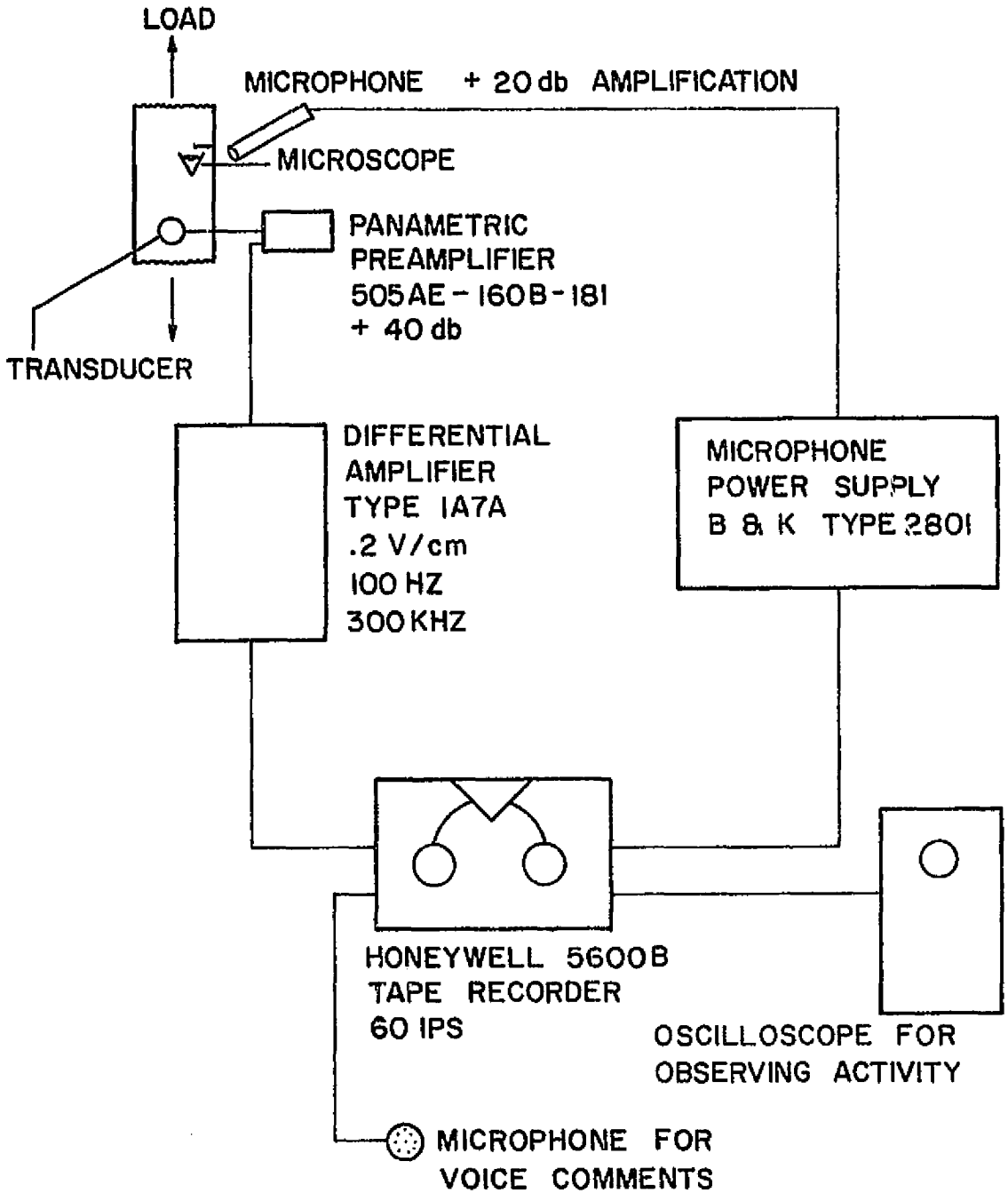

Figure 2. Electrical Equipment for Recording Acustic Emissions

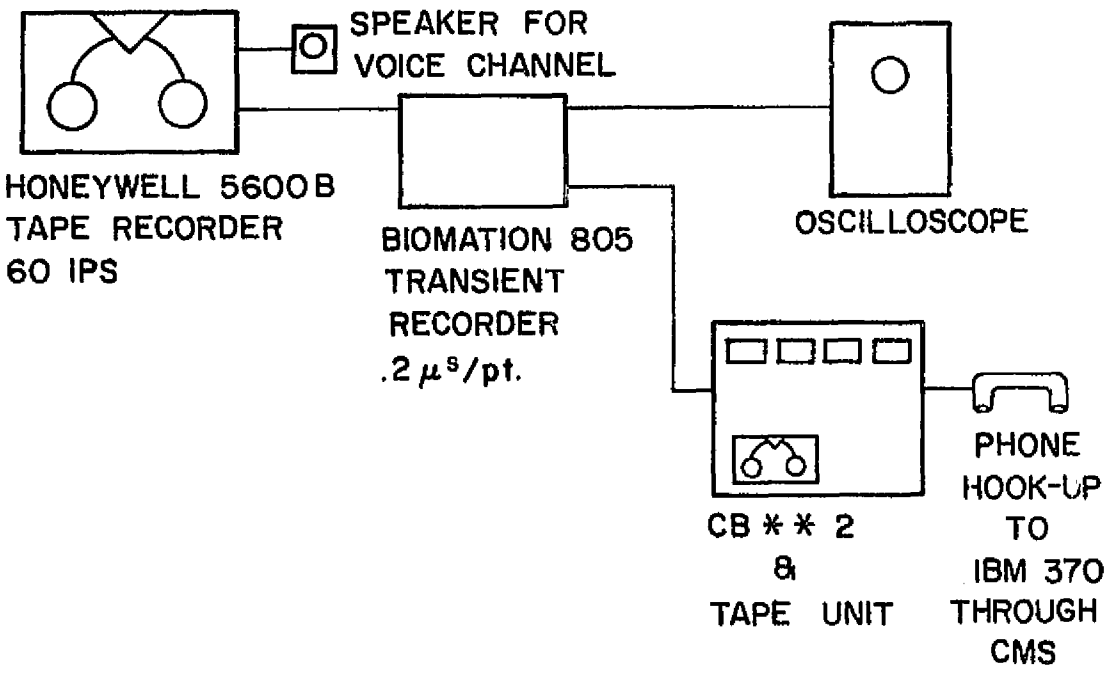

Figure 3. Electrical Equipment for Selecting, Digitizing, and Transmitting Data to Computer

oscilloscope was also connected to visually monitor the emissions. Figure 2 is a schematic diagram of the equipment used to record the signals.

After a series of tests were performed the acoustic emissions were digitized by a Biomation 805 waveform recorder that was interfaced to a microprocessor unit (CB**2) [19-20]. The digitizing interval used was usually .2 microsec/point. Since there are 2048 points of storage available on the recorder this resulted in a signal 409.4 microsec. in duration. The digital signal was stored on the microprocessor's tape unit. When a group of signals were on the tape unit, the microprocessor was interfaced with the central IBM 370 and the signals were transmitted to storage in the IBM 370 and punched on cards for later analysis by a computer program. Figure 3 is a diagram of this system.

As a guide to the response of the transducer, a Bruel and Kjaer type 4138 condenser microphone was used with a Bruel and Kjaer preamplifier type 2618 on a +20 dB sensitivity range. The preamplifier was connected to the tape recorder through a Bruel and Kjaer microphone power supply type 2801. This microphone had a response curve that is almost completely linear from 20 Hz to 225 KHz, and thus could be used as a guide to the response of the transducer by capturing the same signal.

Throughout the project the effect of the frequency response of the transducers on the recorded emission signals remained a perplexing problem. The frequency response could be obtained if the mode of propagation of acoustic emissions were known. The technique is described in reference 21 and requires the use of three transducers.

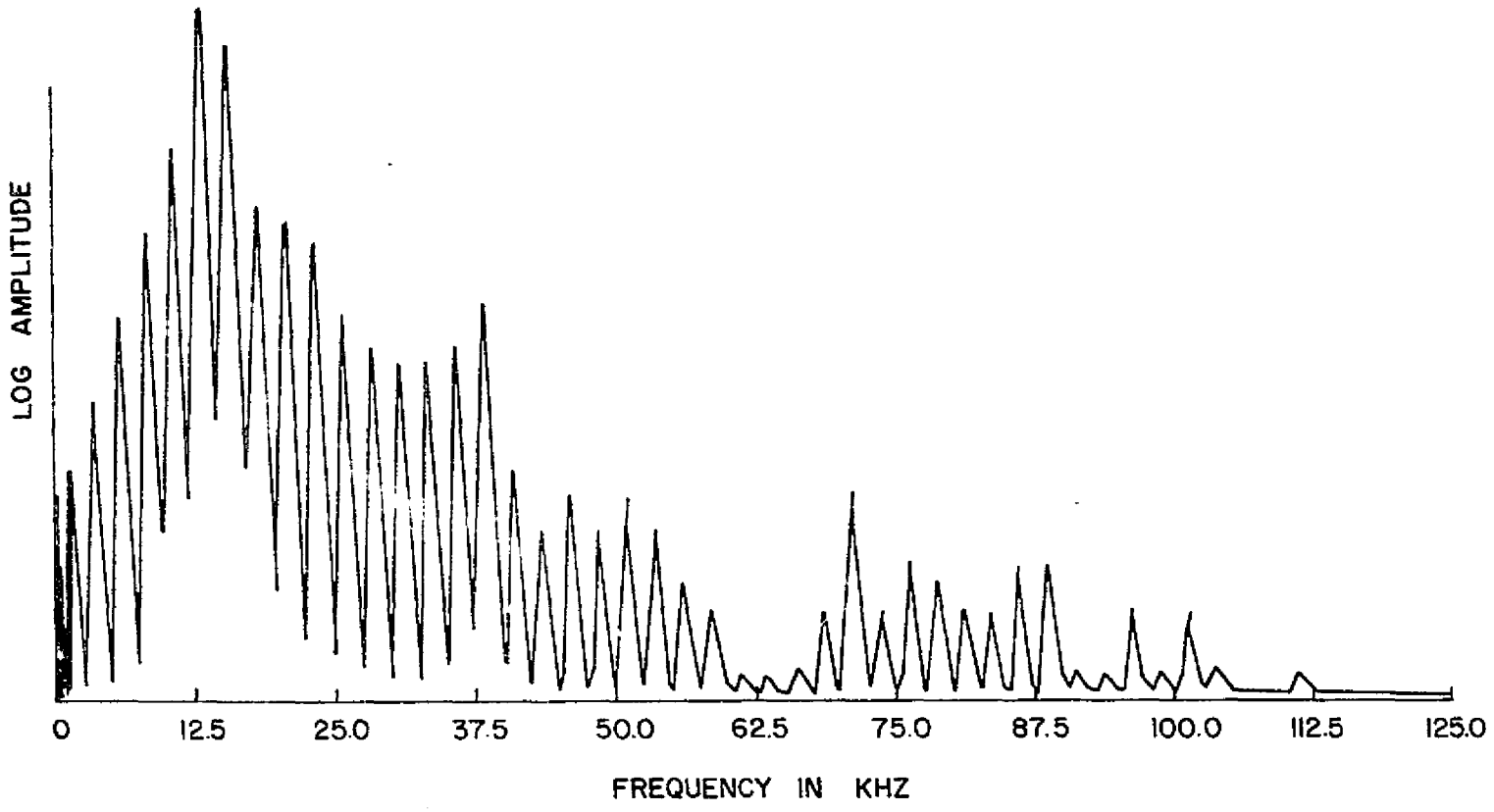

Figure 4. Frequency Response of Panametrics 5070AE 0.1 CC Transducer using Coarse Sandpaper for Excitation

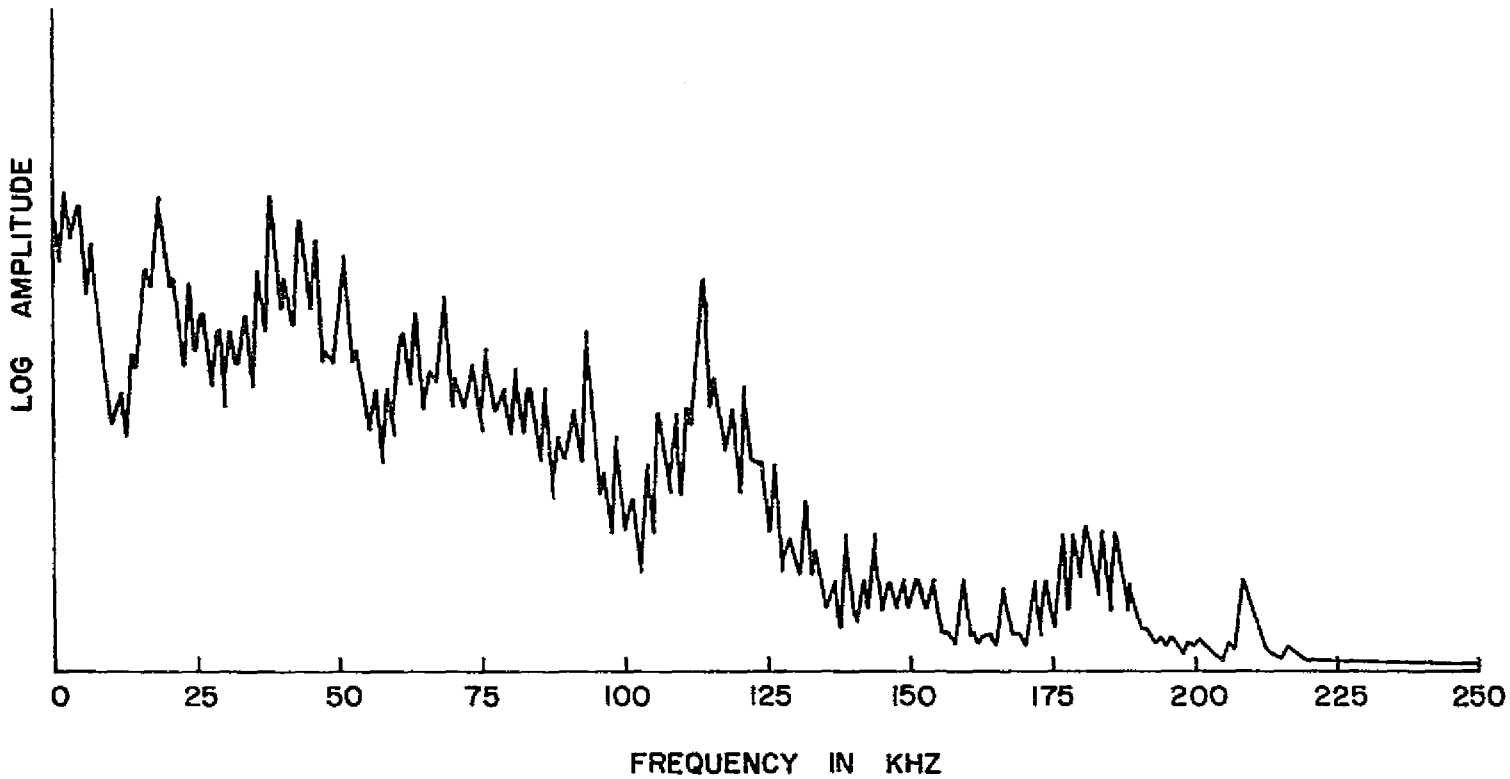

Figure 5. Frequency Response of FAC500 Transducer using Coarse Sandpaper for Excitation

Since the exact mode of propagation of an acoustic emission is not known this technique could not be used here. Instead both the FAC 500 and the 5070AE-0.1 CC Panametrics transducer were bonded on an aluminum beam and the opposite side of the beam was scratched with sandpaper or struck with a small hammer to generate a signal that hopefully was wide band. The resultant signal was analyzed on a Spectral Dynamics real time analyzer. When a particularly wide band signal was obtained, it was graphed as shown in figures 4 and 5. As shown in the figures, neither transducers has a flat response. The Panametrics transducer has a very dominant resonance at 17 KHz. The FAC 500 transducer has a response curve which although not flat is free from very sharp resonances. It was concluded from these tests that although the FAC 500 transducer was not ideal it was much superior to the Panametrics transducer.

Tests were run on the electrical system, excluding the transducers, to obtain a frequency response curve. The results were obtained by introducing a sine wave of known frequency and amplitude into the input of the Panametrics preamplifier and doing analysis on the signal exactly as if it were an acoustic emission. The preamplifier was set at a 40 dB gain, the differential amplifier was set on .2 Volts/cm., and the tape recorder amplification was unity. The tests showed an approximately flat band from 30 KHz to 300 KHz and a total amplification of 45 dB.

Most of the specimens tested were single or three ply graphite-epoxy, 1 inch wide coupons manufactured from prepreg tape on a heated platen press. In addition, several $[0/\pm45/90]_s$ laminates were tested. A number of different types of specimens were made in the effort to

obtain a reproducible fiber failure and matrix crack. The geometry of the specimens helped to determine the dominate failure mode.

Single and three ply 0° specimens with a single crack in the middle of the width or with a short notch cut into the specimen from each edge were tested. The crack and notch were made in several ways. Sometimes a diamond cutting wheel or an exacto knife were used to cut the specimens and sometimes the specimens were laid up before curing with the defects already cut. The usual failure in this type of specimen was for a split to start at the defect and run between the fibers through the matrix material.

A specimen composed of three 90° plys was also tested. In this specimen a crack progressed transversely across the width of the specimen causing a sudden and rapid failure. A frequency analysis of this specimen revealed only very low frequency components. The natural resonances of a broken specimen are expected to be low in frequency. Hence it was concluded that this specimen could not yield information about the fracture process since the natural resonances of the specimen after fracture dominated the acoustic emission.

Finally, a three ply unidirectional $[0_3]$ specimen was made with a gap of approximately one quarter inch in the outer two layers in the center of the gauge length. A notch was started in this gapped section by pricking the middle ply with a knife. This specimen failed by the crack extending across fibers for one eighth to one quarter inch before stopping and then later cracking parallel to the fiber direction exclusively in the matrix. Since only an estimate of the frequency re-

sponse of the transducer-specimen system could be obtained, an exact picture of the acoustic emission could not be achieved. However, if two different failures that are closely spaced in time and in terms of damage to the specimen are analyzed the effect of being viewed through a different specimen response function is minimized. By comparing two closely spaced emissions, qualitative trends may be noted. The three ply $[0_3]$ specimen with one quarter inch gap provided two types of closely spaced emissions. In addition, the transverse crack was mode 1 type fracture while the longitudinal cracking was mode 2 type fracture. Because of these advantages the three ply $[0_3]$ specimen with the gap was primarily used as a source of acoustic emissions to be studied.

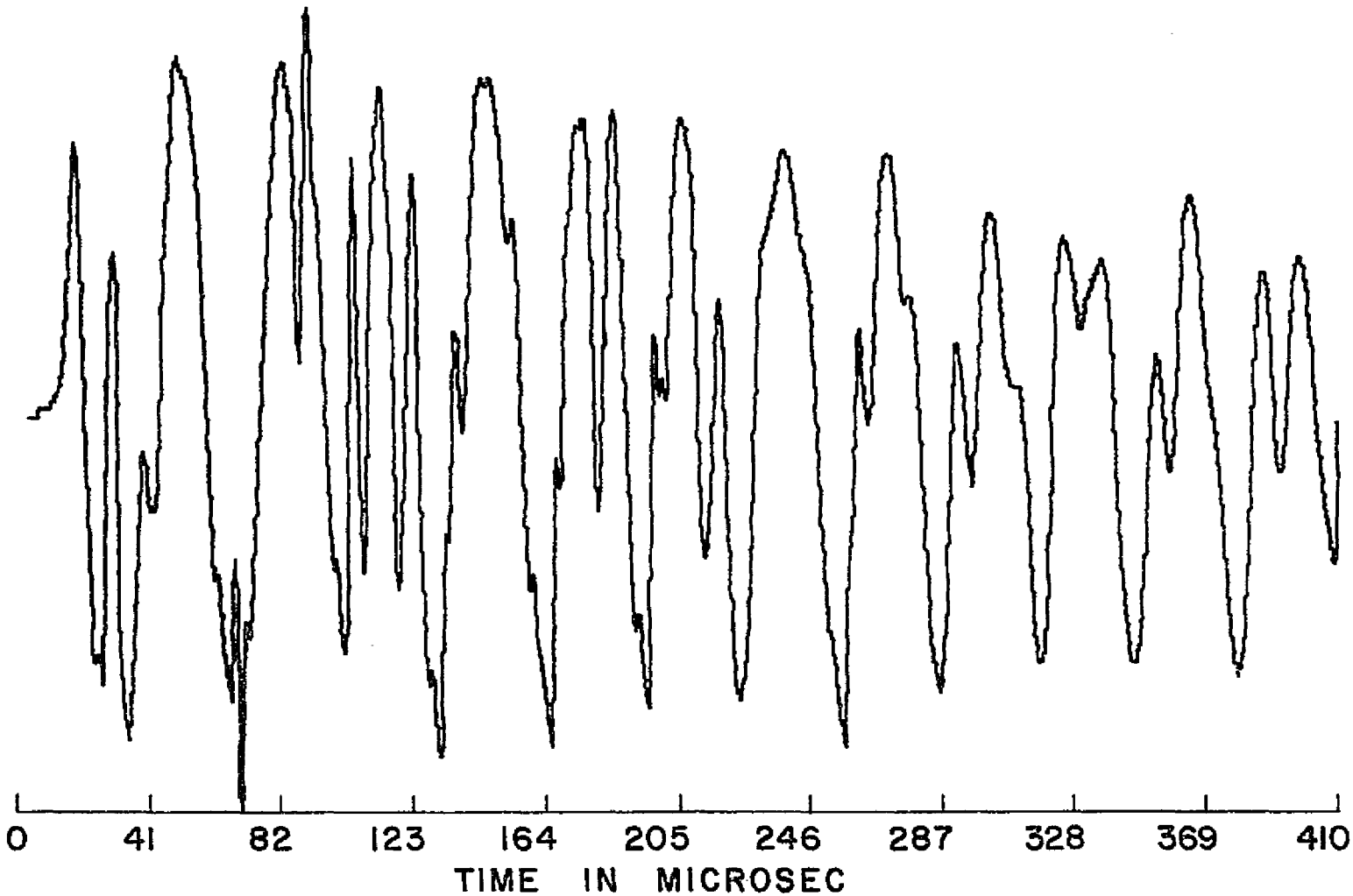

Figure 6. Acoustic Emission from Transverse Crack Growth in $[0_3]$ Specimen, Recorded by Transducer, Normalized with Respect to the Maximum Amplitude of 4.3 volts

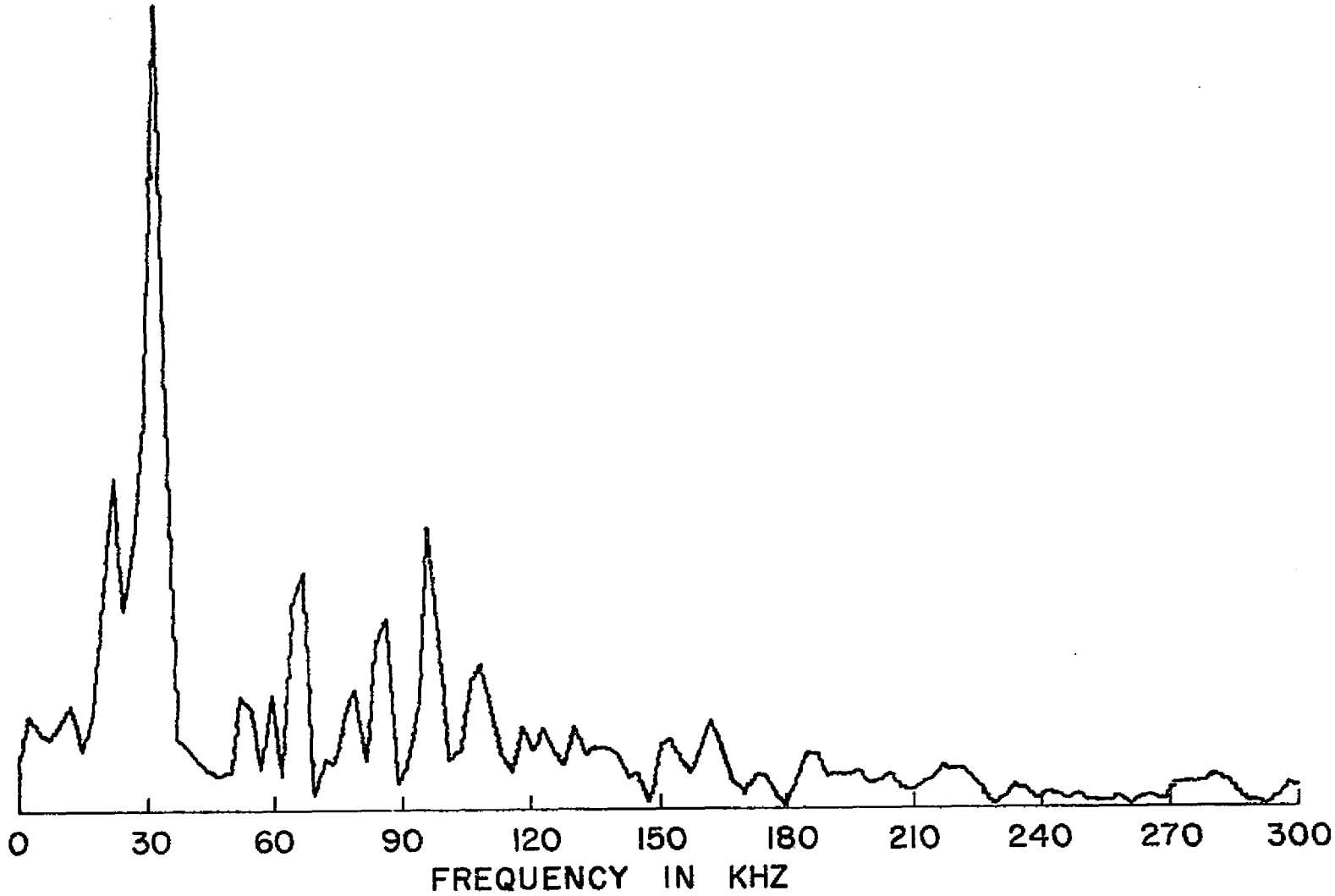

Figure 7. Fourier Transform of Acoustic Emission Shown in Figure 6, Recorded by Transducer from Transverse Crack Growth

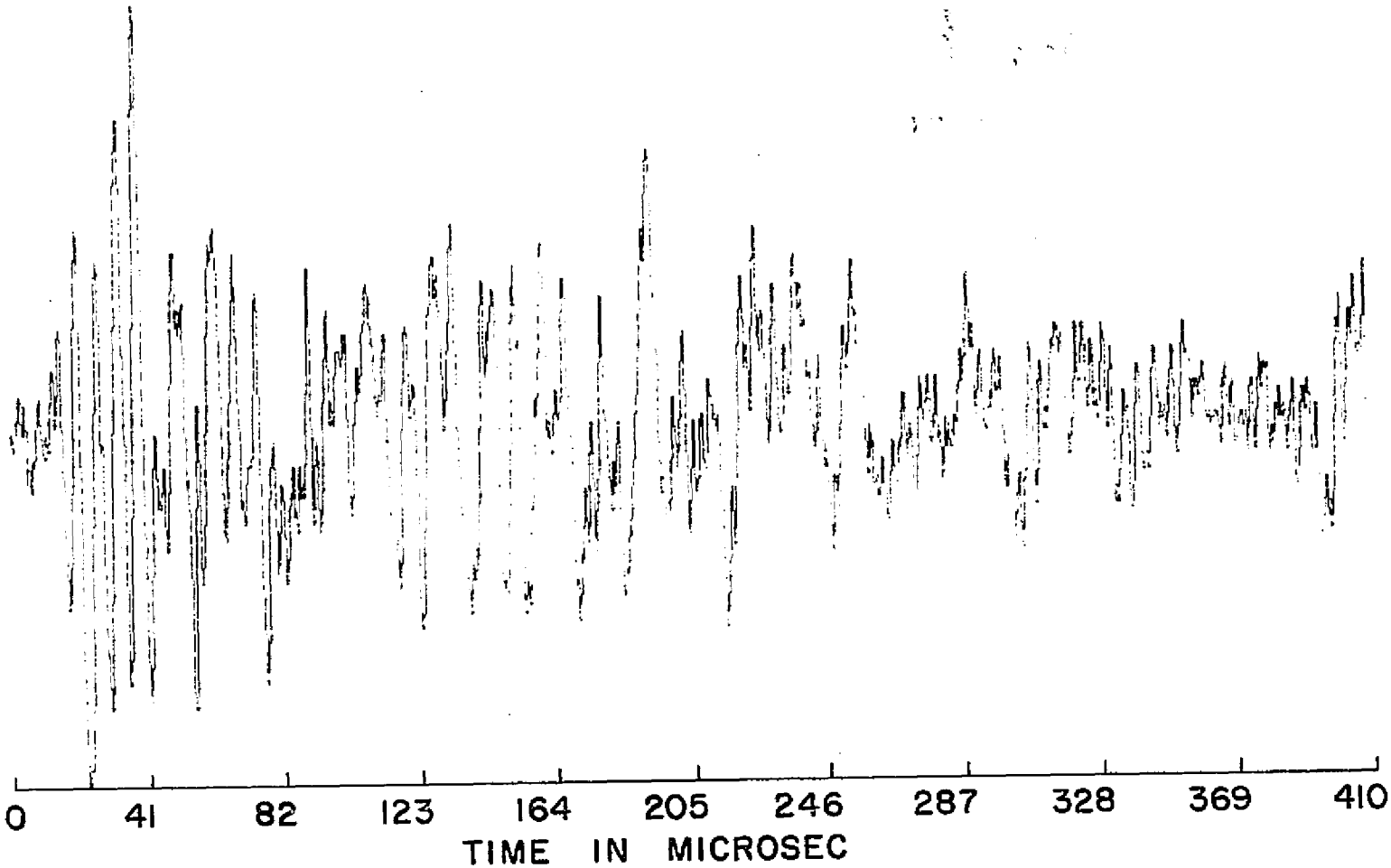

Figure 8. Same Event as Figure 6, from Transverse Crack Growth Recorded by B & K Microphone

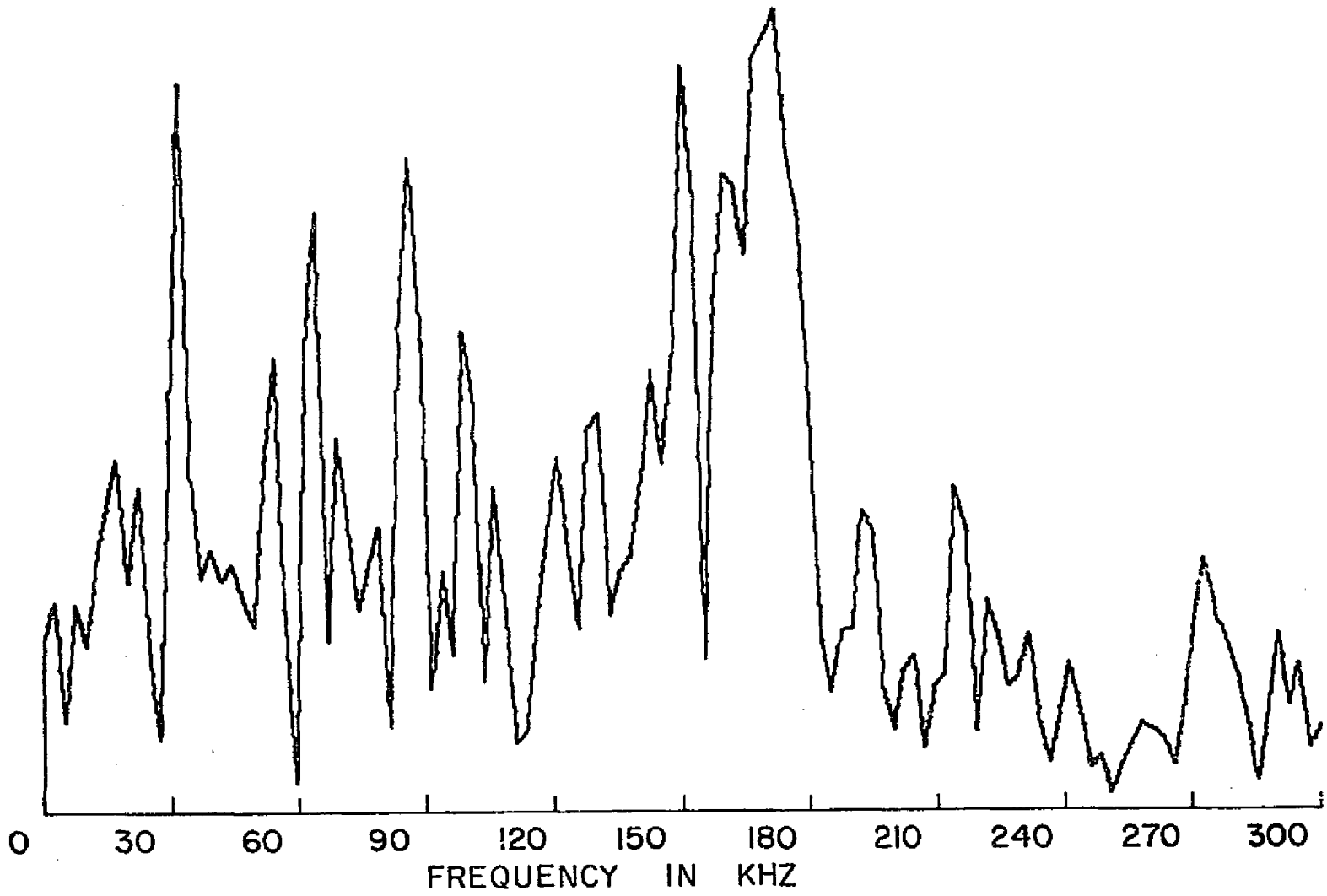

Figure 9. Fourier Transform of Acoustic Emission Shown in Figure 8, Recorded by Microphone from Transverse Crack Growth

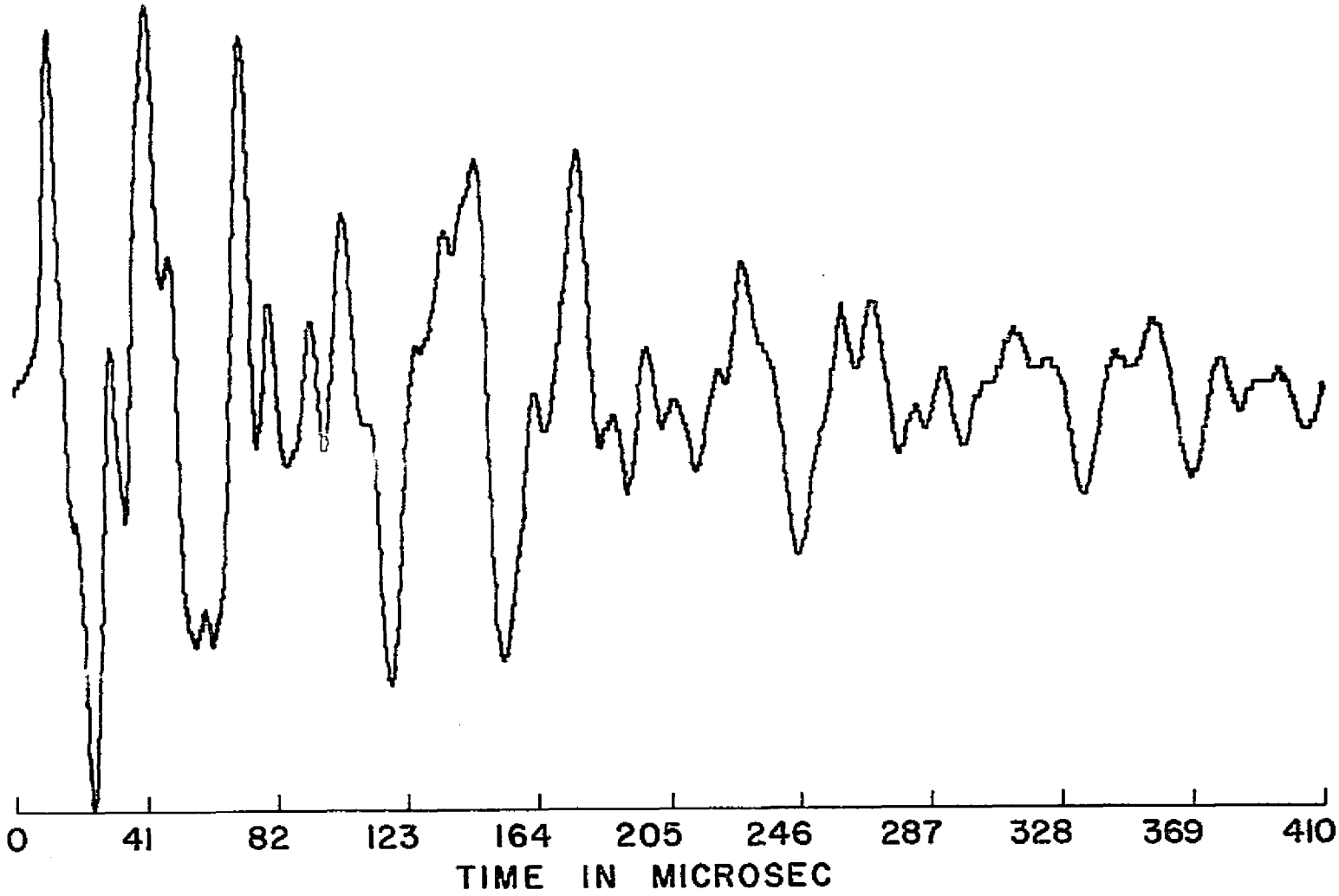

Figure 10. First Acoustic Emission from Longitudinal Crack Growth in $[0_3]$ Specimen, Recorded by Transducer, Normalized with Respect to the Maximum Amplitude of 2.05 volts

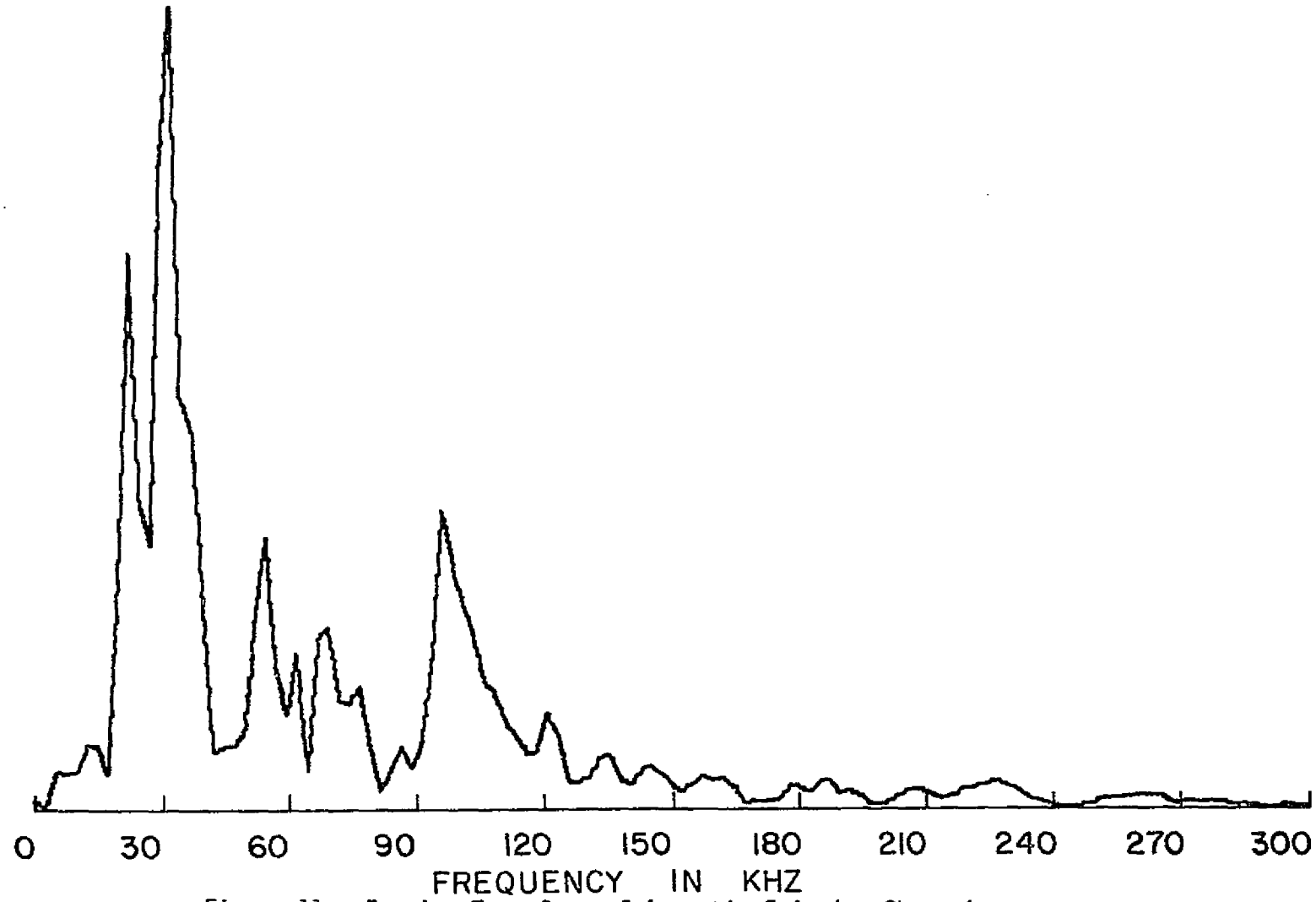

Figure 11. Fourier Transform of Acoustic Emission Shown in Figure 10, Recorded by Transducer, from Longitudinal Crack Growth.

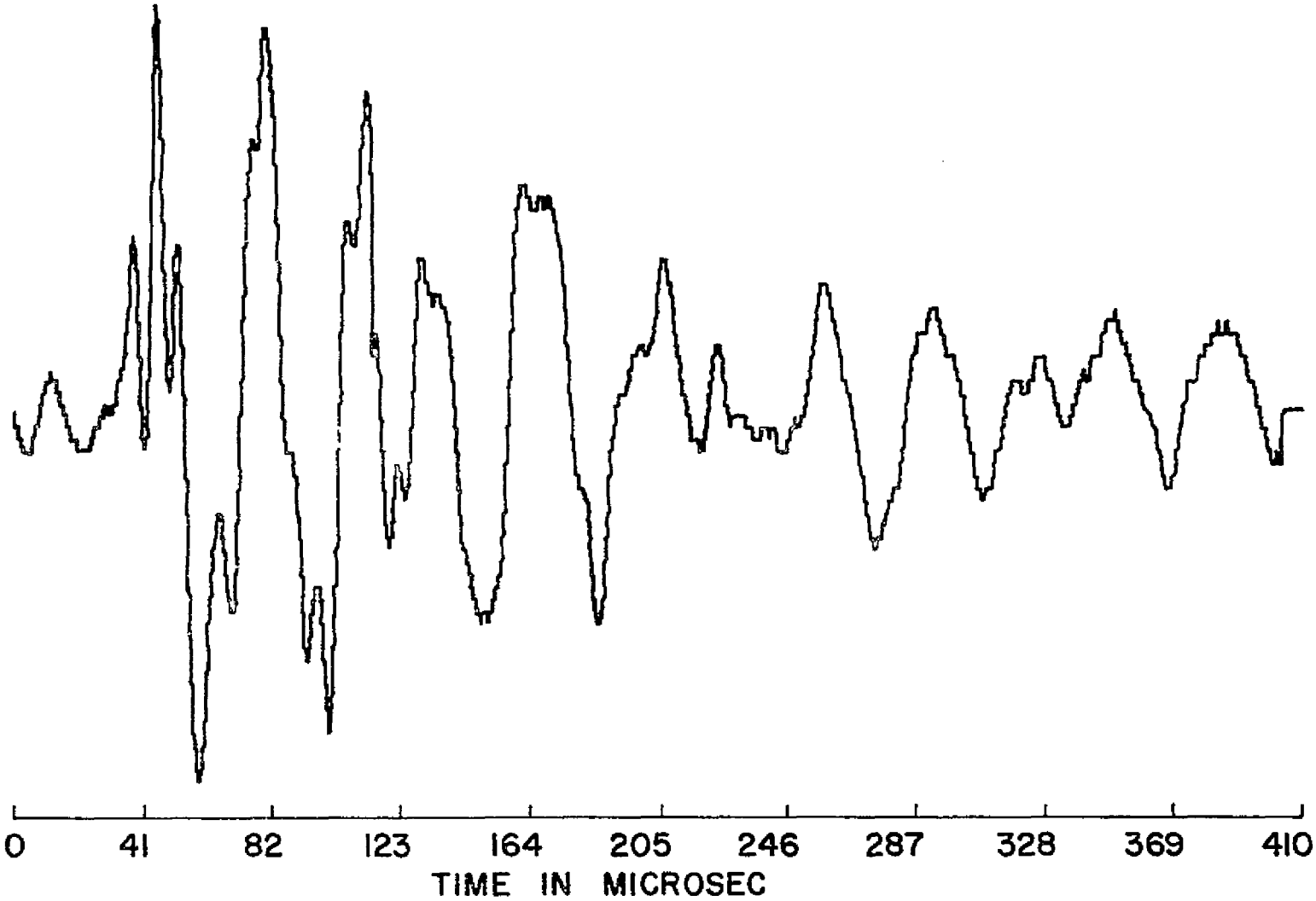

Fig. 12 Second Acoustic Emission from the Longitudinal Cracking of the [0₃] Specimen, Recorded by Transducer, Normalized with Respect to the Maximum Amplitude of 1.7 volts

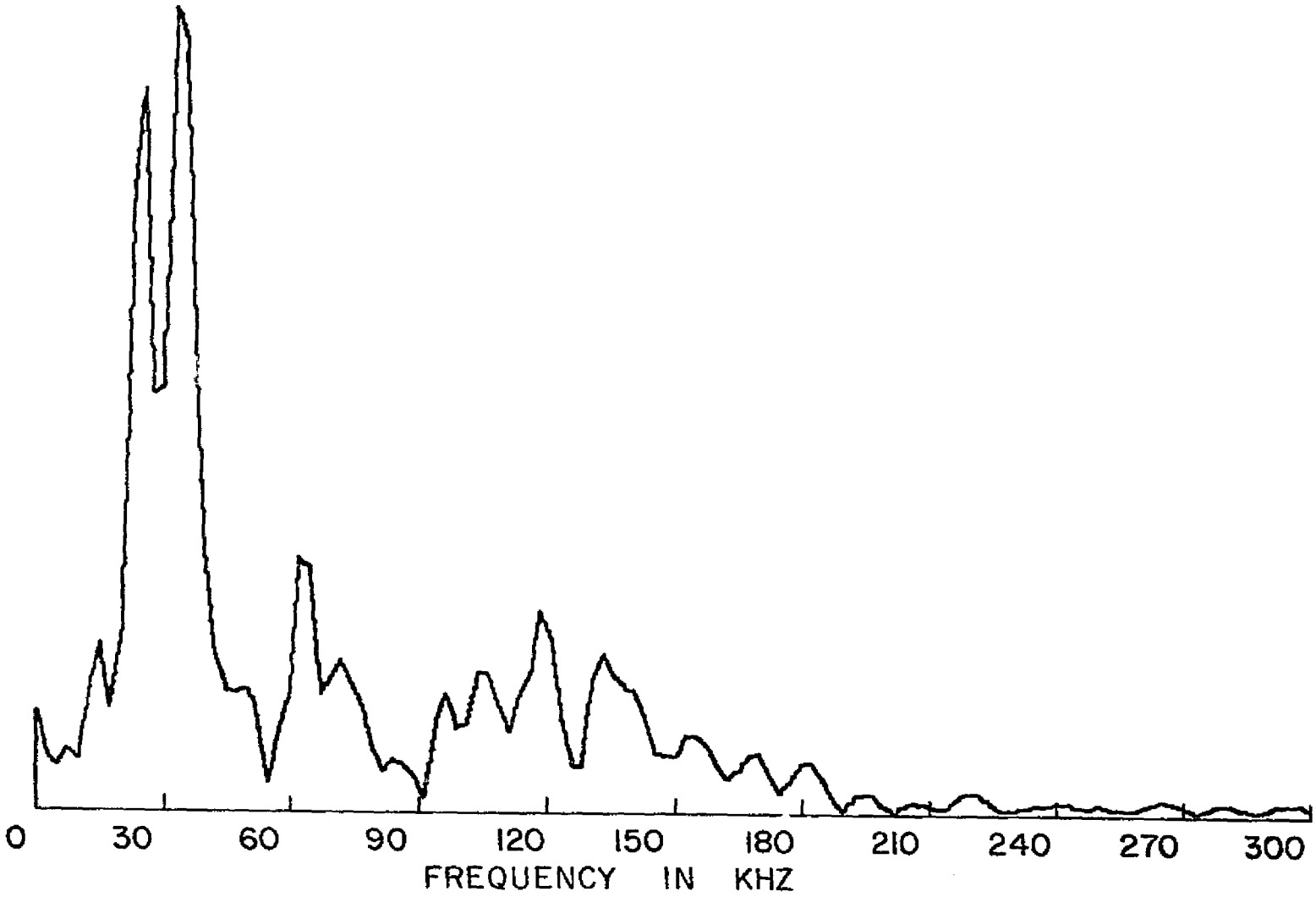

Figure 13. Fourier Transform of Acoustic Emission Shown in Figure 12, Recorded by Transducer from Longitudinal Crack Growth

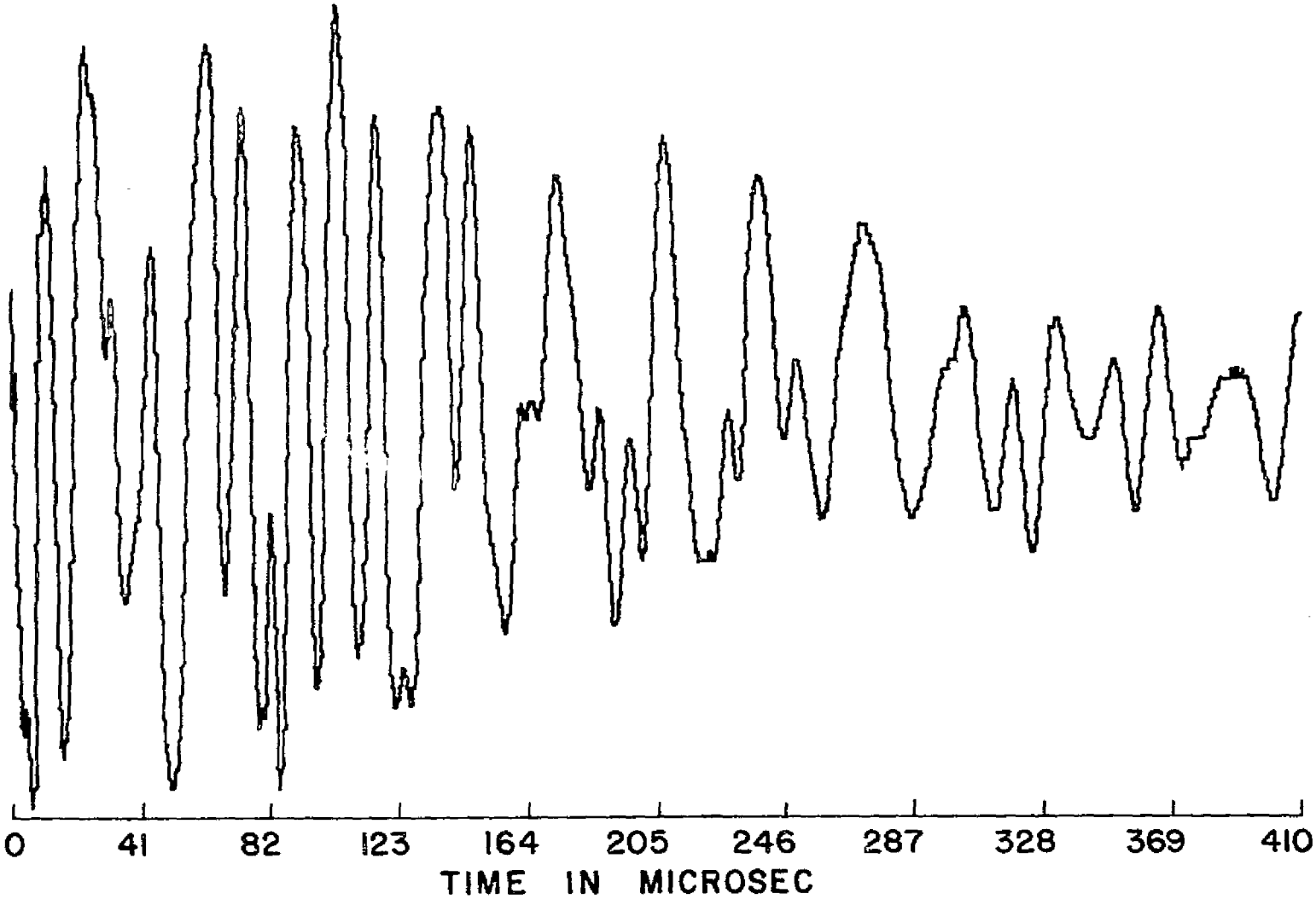

Fig. 14 Acoustic Emission from Longitudinal Crack Growth in the [O_3] Specimen, Recorded by Transducer, Normalized with Respect to the Maximum Amplitude of 3.7 volts

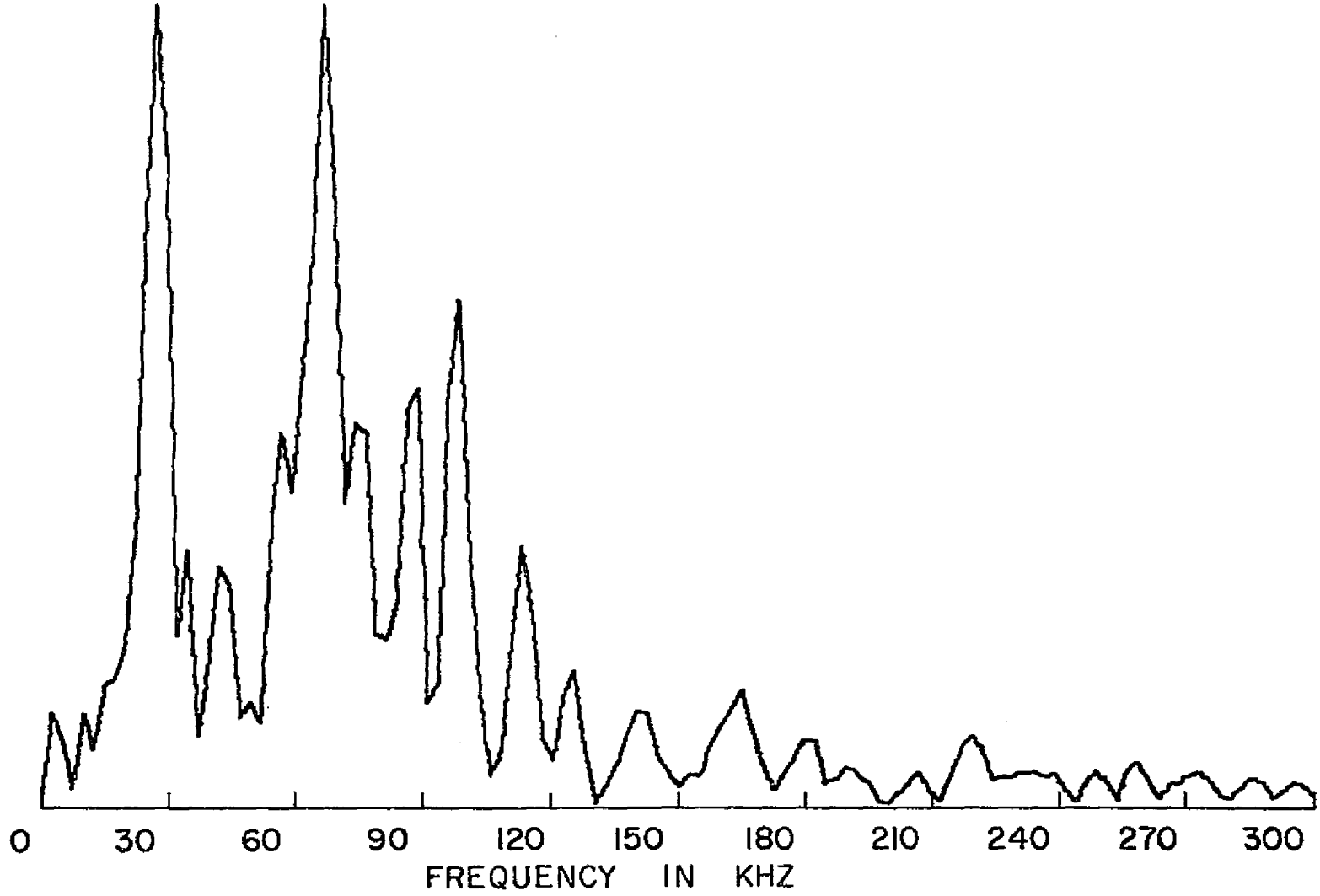

Figure 15. Fourier Transform of Acoustic Emission Shown in Figure 14, Recorded by Transducer from Longitudinal Crack Growth

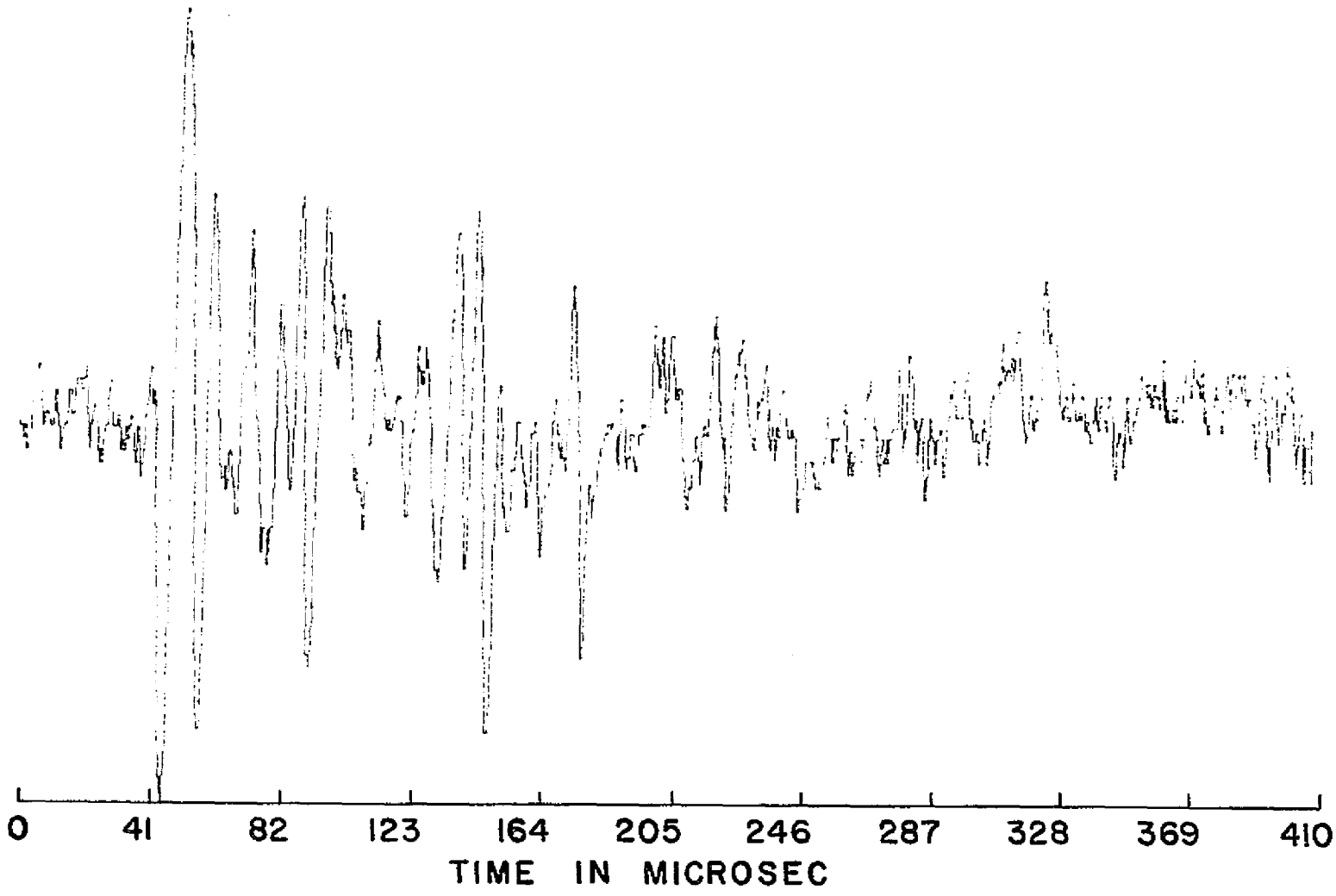

Fig. 16 Acoustic Emission from Longitudinal Crack Growth in the [O_3] Specimen, Recorded by B & K Microphone, Normalized with Respect to the Maximum Amplitude

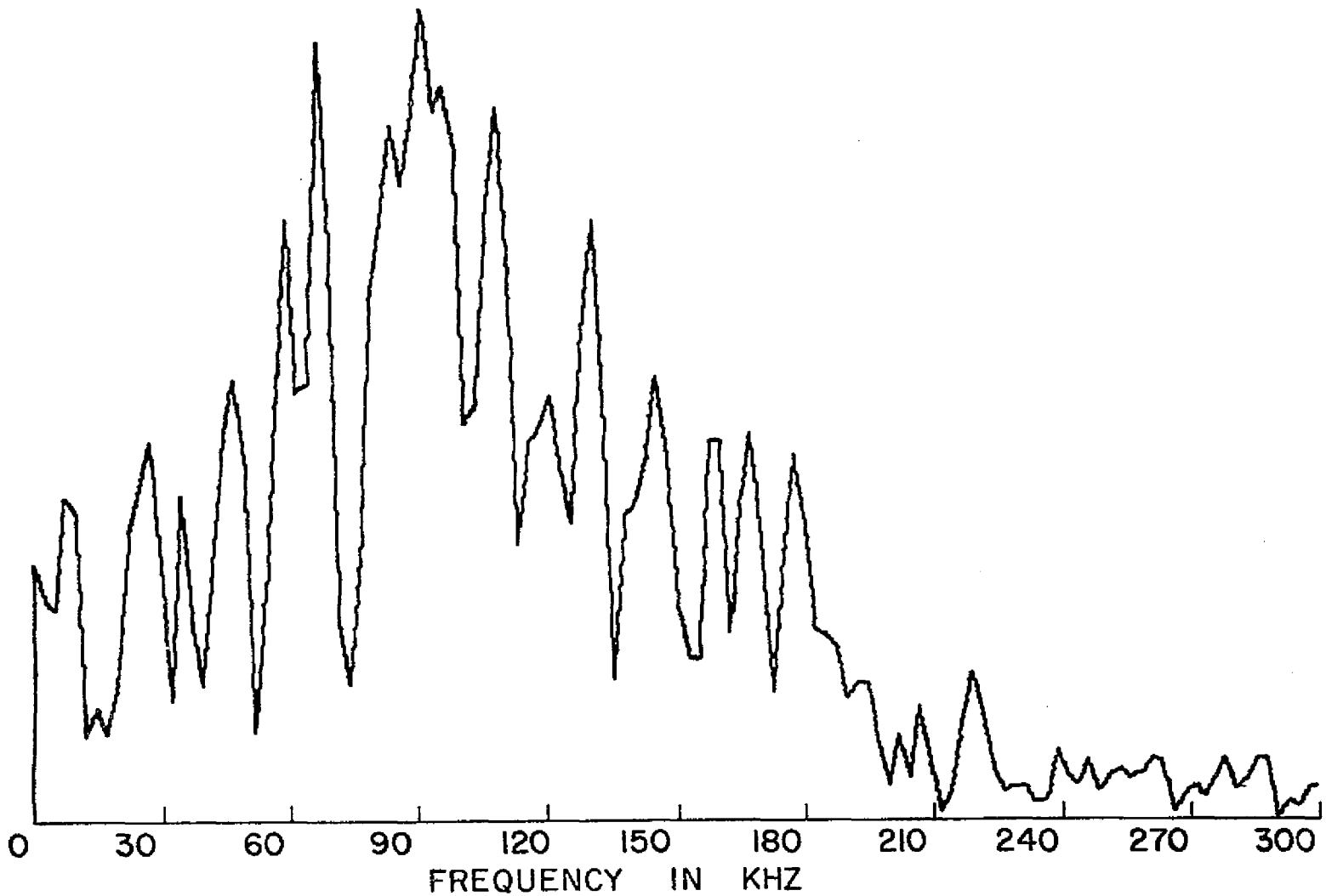

Figure 17. Fourier Transform of Acoustic Emission Shown in Figure 16, Recorded by Microphone from Longitudinal Crack Growth

4. RESULTS

During the course of the experimental work many $[0_3]$ specimens, with the center ply being the only continuous ply, were tested with different gauge lengths. It was hoped that by varying only the length the vibration characteristics of the specimens would be changed, and, therefore, the frequency analysis of the acoustic emissions would change except for possibly some detail that would remain constant and hence characteristic to the failure mode being studied. This line of study was unproductive in revealing the characteristic details of emissions from various types of failure. However, when a comparison of several acoustic emissions from the same specimen is made some patterns are apparent. Figures 6-17 are examples of the acoustic emission signals and their frequency transformed counterparts. The even numbered figures are the acoustic emissions in the time domain and the odd numbered figures are the respective fourier transform. All of these emissions emanated from the same $[0_3]$ ply specimen and were simultaneously recorded through the microphone and the transducer, with the exception of emissions shown in figures 11 and 13 since these had too low an energy to be heard through the microphone.

In this particular test the first fracture was a one quarter inch crack that grew transversely across the fibers from the notch of the initial crack. Figures 6-9 are the data obtained for this event. Figures 6 and 7 were recorded through the transducer and Figures 8 and 9, through the microphone. It should be emphasized that these figures are

the same acoustic emission. The difference in appearance between Figure 6 and Figure 8 is believed to be due primarily to the difference in the response of the transducer and the microphone (as discussed below). This acoustic emission was very loud in comparison with the other emissions. When recorded through the transducer and recorded on the taperecorder this emission had an amplitude of 4.3 volts. As can be seen in Figure 6, this emission took more than 80 μsec. for the amplitude to rise to the maximum peak. The decay of this emission was slow. The amplitude remained large within the 409 μsec. window used for viewing the emission.

Figures 7 and 9 are the frequency transform of this emission as captured through the transducer and microphone respectively. These two figures serve well in contrasting the differences in the response of the transducer and the microphone. The transducer appears to respond to frequencies from 20 to 110 KHZ and drastically filter out all other frequencies. It is likely that the transducer was simply acting as an accelerometer. The relatively large mass of the transducer did not allow it to vibrate at the higher frequencies.

Figures 10-17 are acoustic emissions and their fourier transforms that were apparently from matrix cracking. After the transverse crack propagated across the specimen, there was a short period of quiet when there were no acoustic emissions and no further observed fractures. A crack then formed at the tip of the crack and ran longitudinally in the specimen. This crack emitted several distinct separate emissions and thus must have grown in several bursts. The crack that ran across

the fiber can definitely be tied to a certain acoustic emission because there was only one emission recorded at this time. The growth of the crack longitudinally in the specimen may have crossed misaligned fibers. Because of this, emissions from longitudinal crack growth can not be said to always be due only to matrix breakage. Also because of the number of emissions and equipment limitations it was difficult to distinguish which emission on the tape track recorded through the microphone corresponds to an emission recorded on another track through the transducer. However, the propagation of the crack can be said to have fractured primarily matrix material.

Figure 10 was the first acoustic emission encountered during the growth of this longitudinal crack. The amplitude of this emission was relatively small, measuring only 2.05 volts output from the tape recorder. This particular emission was captured only through the transducer. The shape of this emission was characteristic of most of the emissions thought to be caused by matrix cracking. This emission rises to a maximum amplitude at the very first and then rings down along a rapidly decaying sinusoidal. It should be emphasized when inspecting the fourier transform of this emission (Figure 11) that this emission was recorded through the transducer. The frequency representation of emissions recorded through the transducer have higher frequencies somewhat filtered.

The emission pictured in Figure 12 and its fourier transform in Figure 13 followed within one second after the previously discussed emission. This emission likewise was recorded only through the trans-

ducer. The amplitude of this emission at the tape recorder output was 1.7 volts. This signal has the general shape discussed previously as the characteristic pattern for a matrix crack.

The emissions pictured in Figures 14 and 16 occurred either very close together or were the same emission. Because of equipment limitations the two tracks containing the test data from the transducer and the microphone have to be reviewed one at a time. When these emissions were selected for analysis it was thought they were the same emission. The first of these two was recorded through the transducer at an amplitude level of 3.7 volts output from the tape recorder. The second emission was monitored via the microphone. The emission shown in Figure 14 does not follow the pattern of most matrix crack type emissions exactly. The amplitude of this emission remains at a high level for 120 μsec. and then decays in a manner similar to the previously discussed matrix crack pattern. A possible explanation for this behavior is that the crack ran for some distance in the material adding energy at a more or less constant level to the emission. This would also help to explain the large amplitude from a type of failure characterized by low amplitude acoustic emissions. Figure 15 is the frequency transform of this emission. The amplitude and number of peaks between 50 KHZ and 115 KHZ should be noted. For most emissions originating from matrix cracking a larger portion of the energy of the emission appears to be in this frequency range.

The emission pictured in Figure 16 more closely follows the pattern for a matrix crack emission. A comparison of the frequency transform of

this emission with the last emission (Figure 17 and 15) reveals that while most of the peaks occur at the same frequency level there is a vast difference in the amplitudes of the peaks between the two signals. The frequency representation of the emission shown in Figure 16 is a better indication of the frequency composition of a matrix cracking type of emission since it was obtained through the microphone. The majority of the energy of this emission seems to be between 50 KHZ and 150 KHZ.

Acoustic emissions from a matrix cracking failure event usually are relatively low in amplitude. There are exceptions as in Figure 14. However, for the exceptions the crack ran rapidly for an unusually long distance. The high amplitude could be due to the crack propagating at a speed equal to the wave speed in the material. If this happened energy released from the crack would be added to the acoustic emission at the very first wavefront, that is, energy is added until a large amplitude emission is obtained. The emission from a matrix crack appears to be a single impulse that decays rapidly. This emission starts by rising to its maximum amplitude almost immediately relative to a 400 μsec. time frame. The emission usually has decayed to the background noise level before the end of the 400 μsec. time frame. In the frequency domain these emissions are characterized by large portions of energy between 50 KHZ and 150 KHZ.

The most notable feature of acoustic emissions from fiber breaks is the relatively large amplitude. Acoustic emissions from fiber breaks are usually twice as loud as acoustic emissions from matrix cracking in the specimens tested in this study. These emissions start at less than

the maximum amplitude of the emission. Usually 40 to 100 μsec. after the start of the emission the largest peak occurs. The amplitude declines only slightly in a 400 μsec. time frame. A possible explanation for this behavior is that the crack velocity is much slower than the wave speed in the material. As the crack moves across new fibers, new energy is added at a slow rate until the crack progress is halted. This may be due to a pause of the crack growth for a very small period of time at a fiber until finally the fiber is ruptured. Acoustic emissions from crack growth across fibers have large amounts of energy in the 50 to 190 KHZ range. It must be remembered that this type of crack growth contains both fiber and matrix failure. The new band of frequency components not present in matrix cracking must be due to the fiber breakage. Especially large amounts of energy from 140 KHZ to 180 KHZ must be due to fiber breakage.

Throughout these tests the major unresolved problem has been the effect of the frequency response of the transducer and the mechanical resonances of the specimen on the recorded acoustic emission signal. The frequency content of any emission is largely determined by the natural responses of the specimen and the transducer. Both the specimen and the transducer act as a medium for the transmission of information. However, the responses of both elements are not flat or simple curves, but have peaks that emphasize some portions of a signal. If a combined response curve for the transducer-specimen system could be obtained, the information within an acoustic emission might yield more complete characteristics of different types of failure. The usual experimental

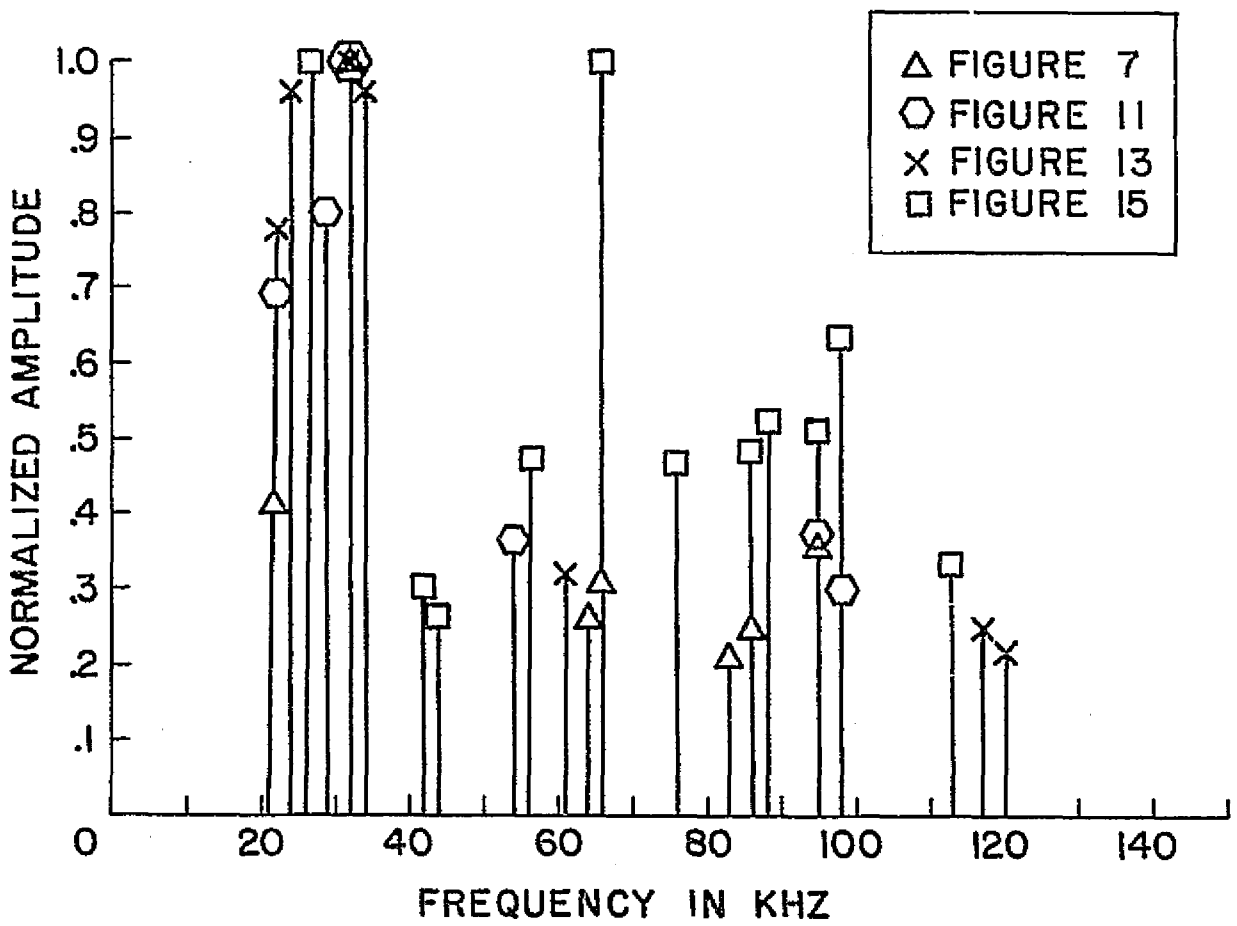

Figure 18. Peaks of the Fourier Transformed Acoustic Emissions Shown Previously from the $[0°]_3$ Specimen, Recorded by the Transducer

method for obtaining a response curve is to strike the specimen with a hammer which has an accelermoeter attached and to divide the fourier transformed signal from the transducer by the fourier transformed signal from the accelerometer. This method could not be used here because the response is sensitive to the location and direction of the applied impulse; and in obtaining the response in this manner, the transducer could easily be debonded from the specimen. That is, the curve obtained would only be applicable for an emission originating exactly at the place hit with the hammer and with a displacement direction in the same direction as the impulse applied by the hammer.

To make the effect of the specimen-transducer resonances clear a graph of the peaks of all the previously discussed fourier transformed emissions obtained through the transducer is included as Figure 18. In this figure the amplitude of the peaks in each transformed emission has been normalized with respect to the amplitude of the maximum frequency component in that particular emission. The effect of the natural system resonances can be seen by the occurence of many data points along single frequency lines.

The advantages of using a microphone instead of a transducer are many. The Bruel and Kjaer type 4138 microphone has good response characteristics from 20 HZ to over 200 KHZ. Using a microphone, no physical contact with the specimen is necessary. The response characteristics of the specimen are not affected by the method of detection. It may be practical to obtain experimentally a natural response curve of the specimen alone by an impact method similar to that des-

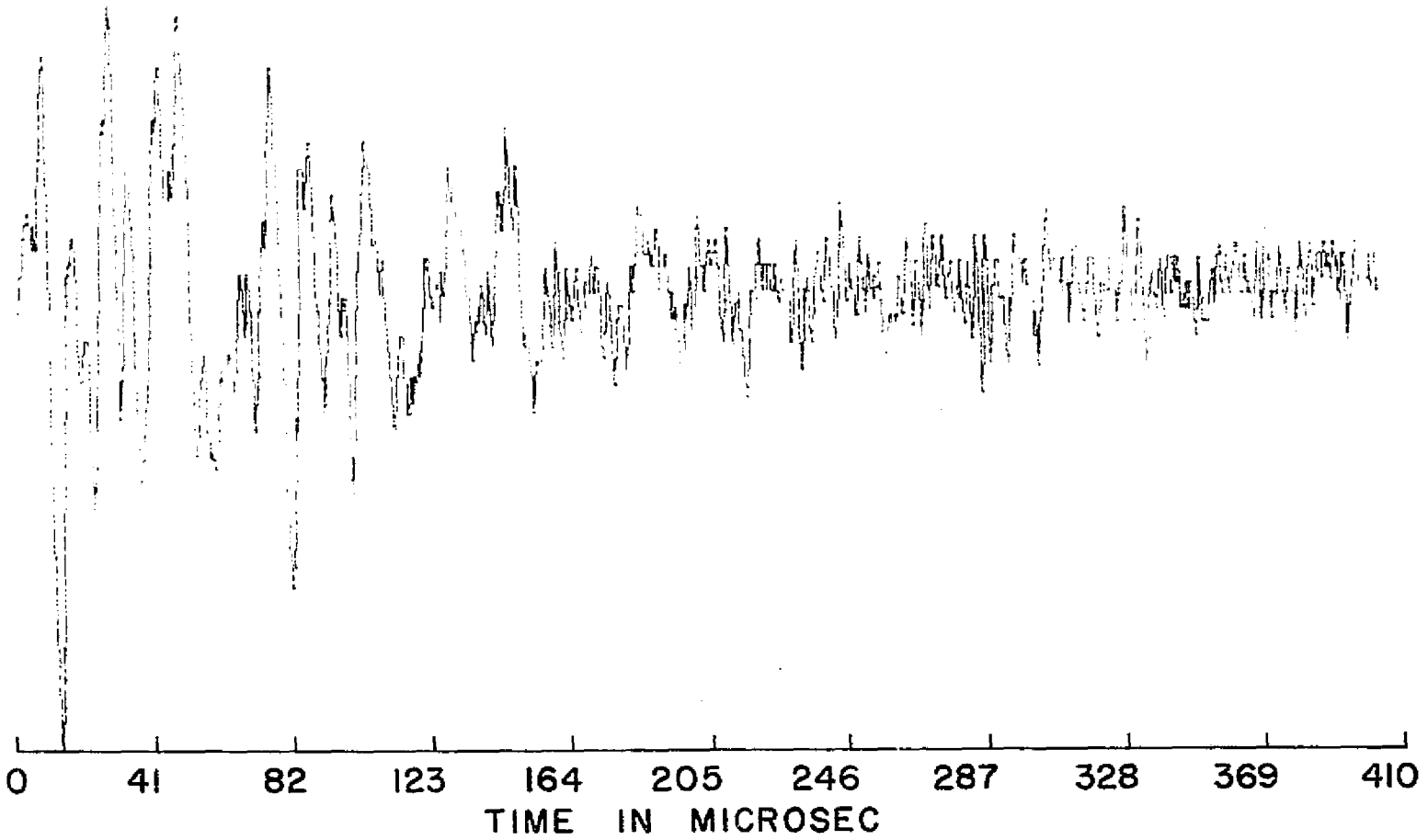

Figure 19. Acoustic Emission from the $[0/\pm45/90]_s$ Specimen at 1050 lbs. Load, Recorded by Transducer, Normalized with Respect to the Maximum Amplitude

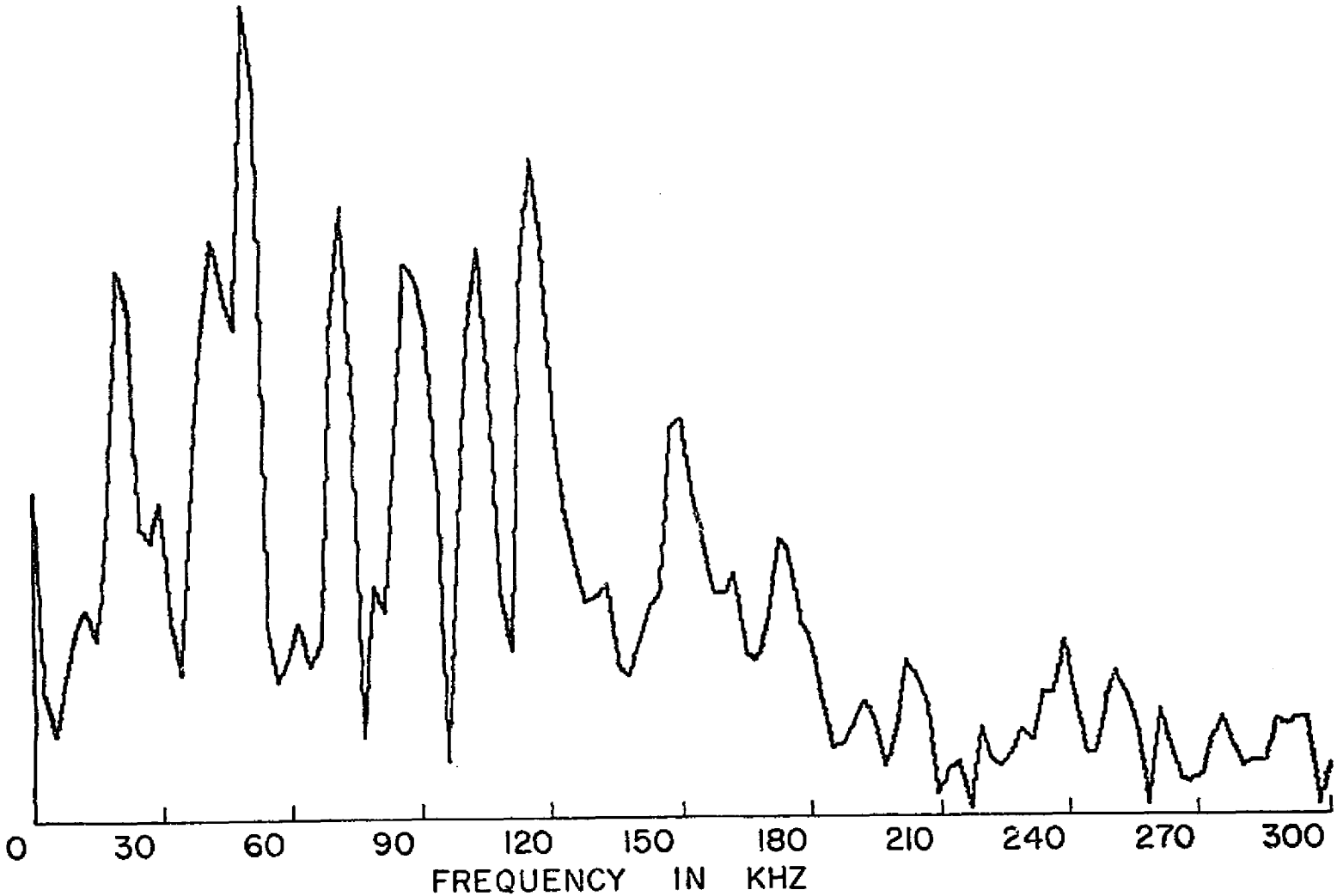

Figure 20. Fourier Transform of Acoustic Emission Shown in Figure 19, Recorded by Transducer from the $[0/\pm45/90]_S$ Specimen at 1050 lbs. Load

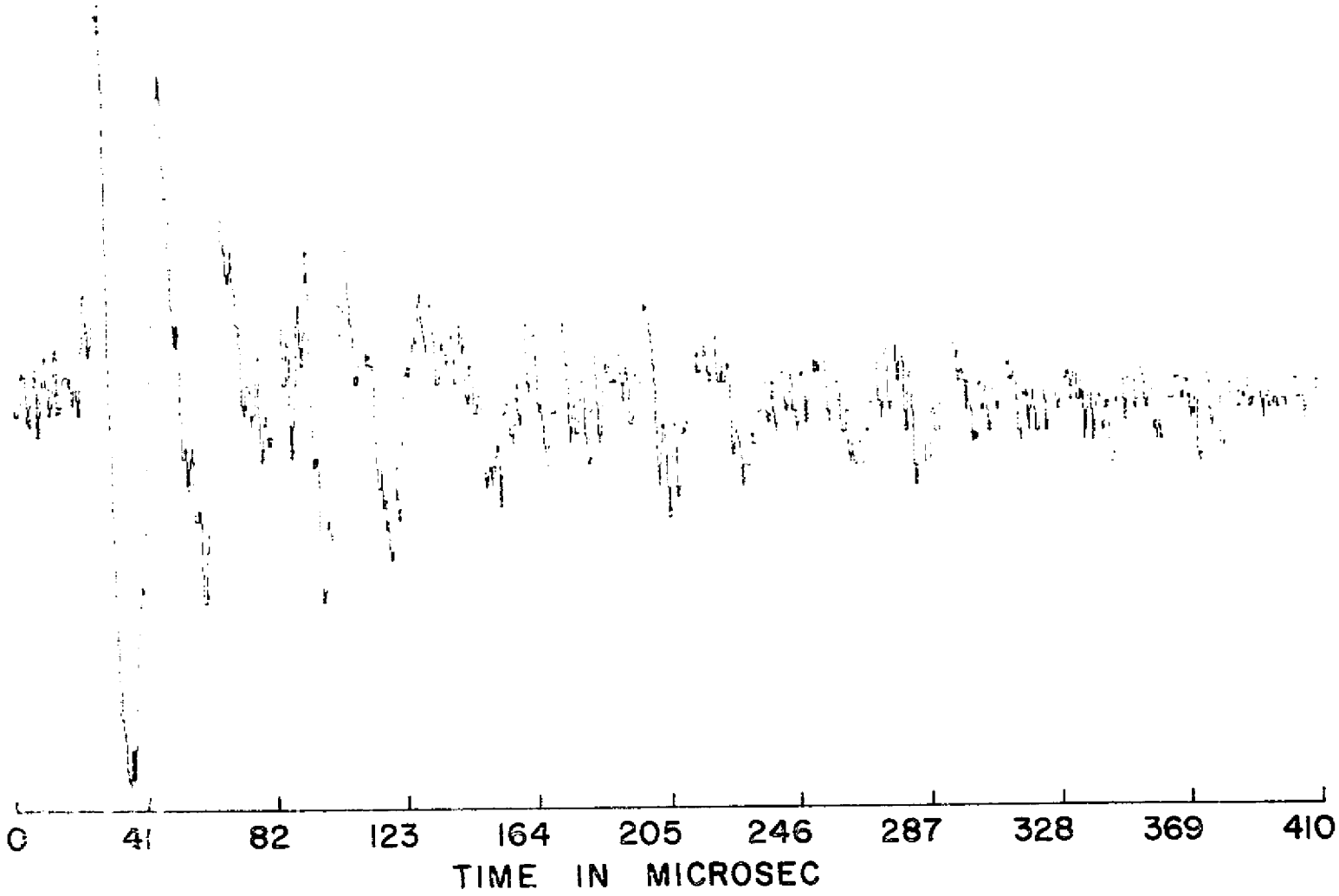

Fig. 21 Acoustic Emission from the $[0/\pm45/90]_S$ Specimen at 1450 lbs Load, Recorded by Transducer, Normalized with Respect to the Maximum Amplitude

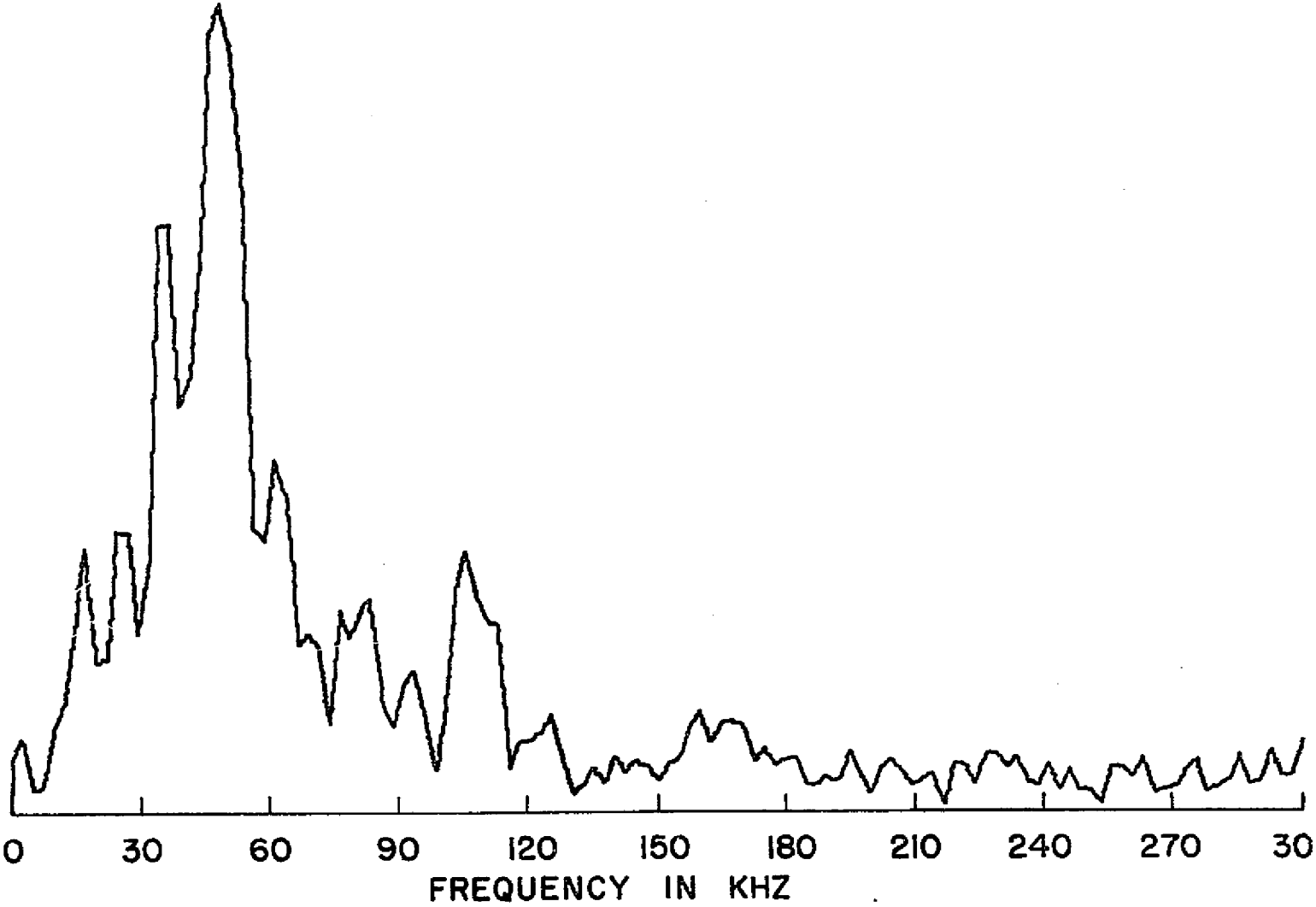

Fig. 22 Fourier Transform of Acoustic Emission Shown in Figure 21, Recorded by Transducer from the $[0/\pm45/90]_S$ Specimen at 1450 lbs. Load

cribed previously if a microphone is used instead of a transducer.

Several acoustic emissions from a specimen were captured simultaneously with the microphone and with the FAC 500 transducer allowing for comparison of the response of the transducer to the flat response of the microphone. Figures 7 and 9 are examples of fourier transforms of an acoustic emission captured simultaneously by the transducer and the microphone, respectively. From a comparison of these and other signals the transducer appears to emphasize the portion of the signal between 20 KHZ and 60 KHZ. The transducer appears particularly poor at responding to frequencies above 110 KHZ.

A single $[0/\pm45/90]_s$, 1x7x0.052 inch, graphite/epoxy coupon specimen was also tested. The damage characteristics of a specimen of this type have been well documented using a replication technique of the specimen edge [22]. Figures 19-22 are two emissions and their fourier transforms monitored for this type of specimen through the transducer. Both of these emissions were recorded with the load level well below 1600 lbs. with a maximum amplitude at the tape recorder output of .16 and .19 volts respectively. Because of the low level of these emissions, the microphone did not respond to them. Figures 19 and 22 reveal a signal that reaches a maximum amplitude very rapidly and decays to the background noise level very quickly. According to the study of damage processes in this specimen at load levels up to 1600 lb., this specimen is undergoing transverse cracking in the 90° plies [22]. The frequency transform could not be compared with the characteristic frequencies for a matrix cracking type emission since the frequency characteristics are

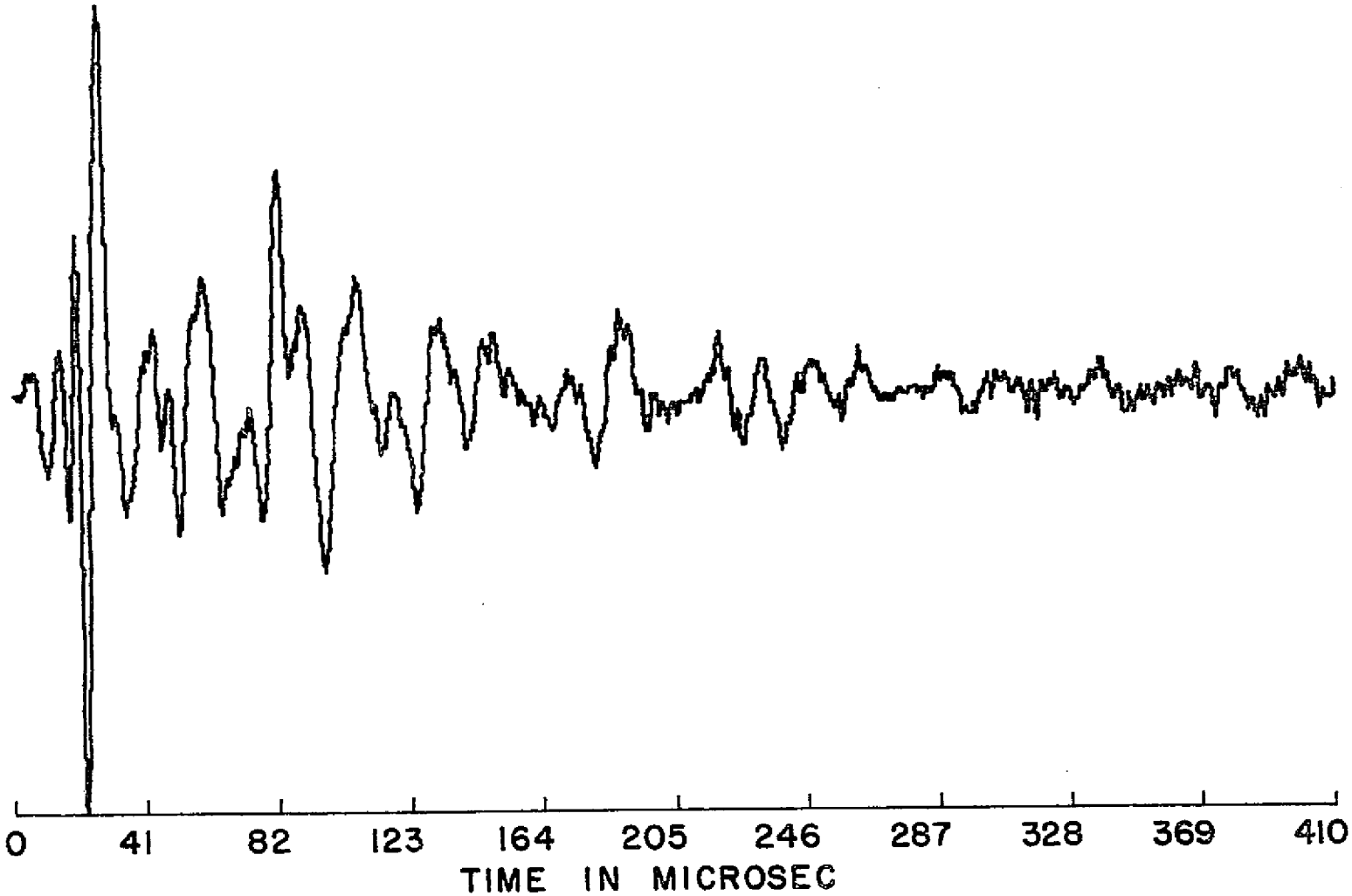

Fig. 23 Acoustic Emission from the $[0/\pm45/90]_S$ Specimen at 1600 lbs. Load, Recorded by Transducer, Normalized with Respect to the Maximum Amplitude

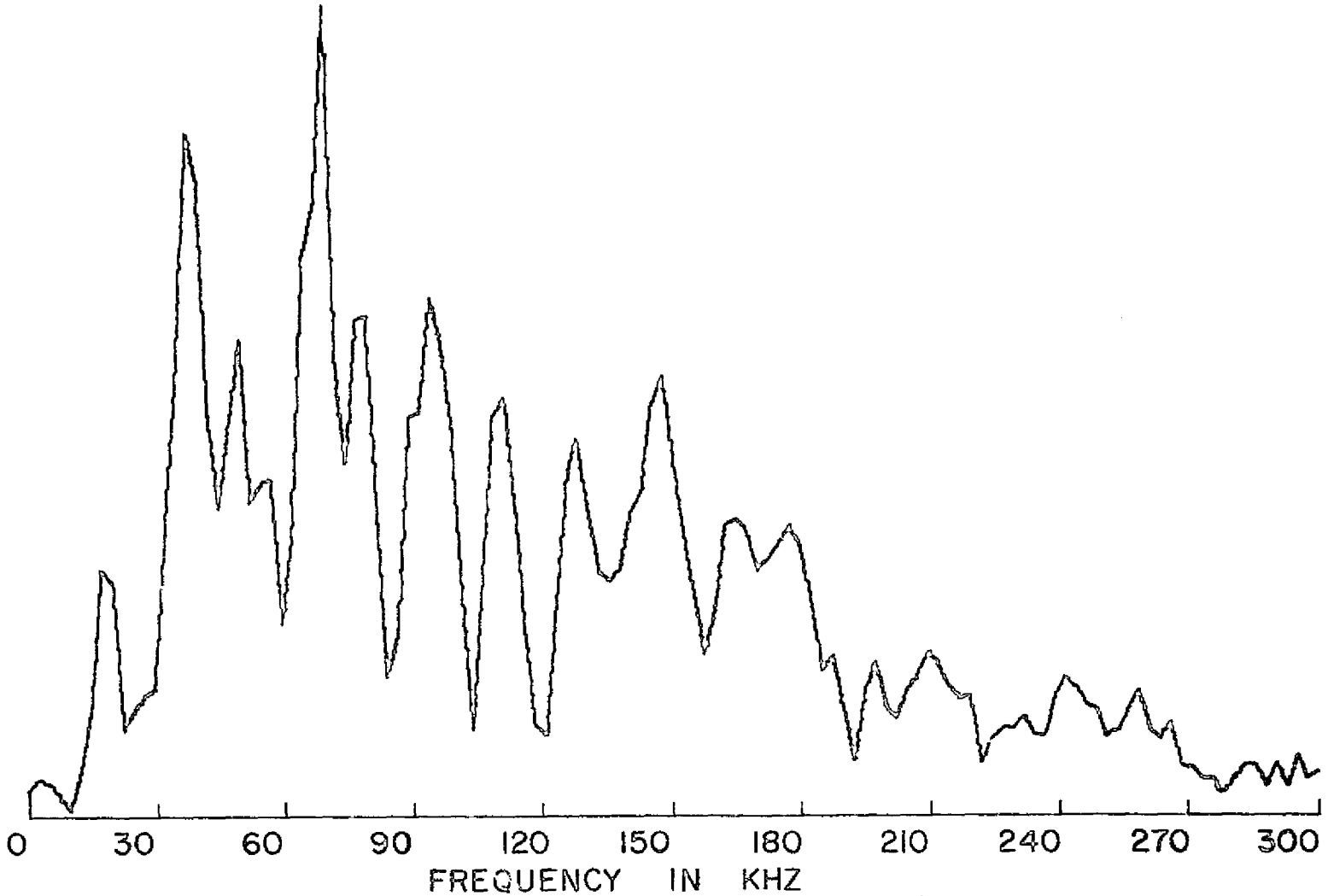

Figure 24. Fourier Transform of Acoustic Emission Shown in Figure 23, Recorded by Transducer from the $[0/\pm45/90]_s$ Specimen at 1600 lbs. Load

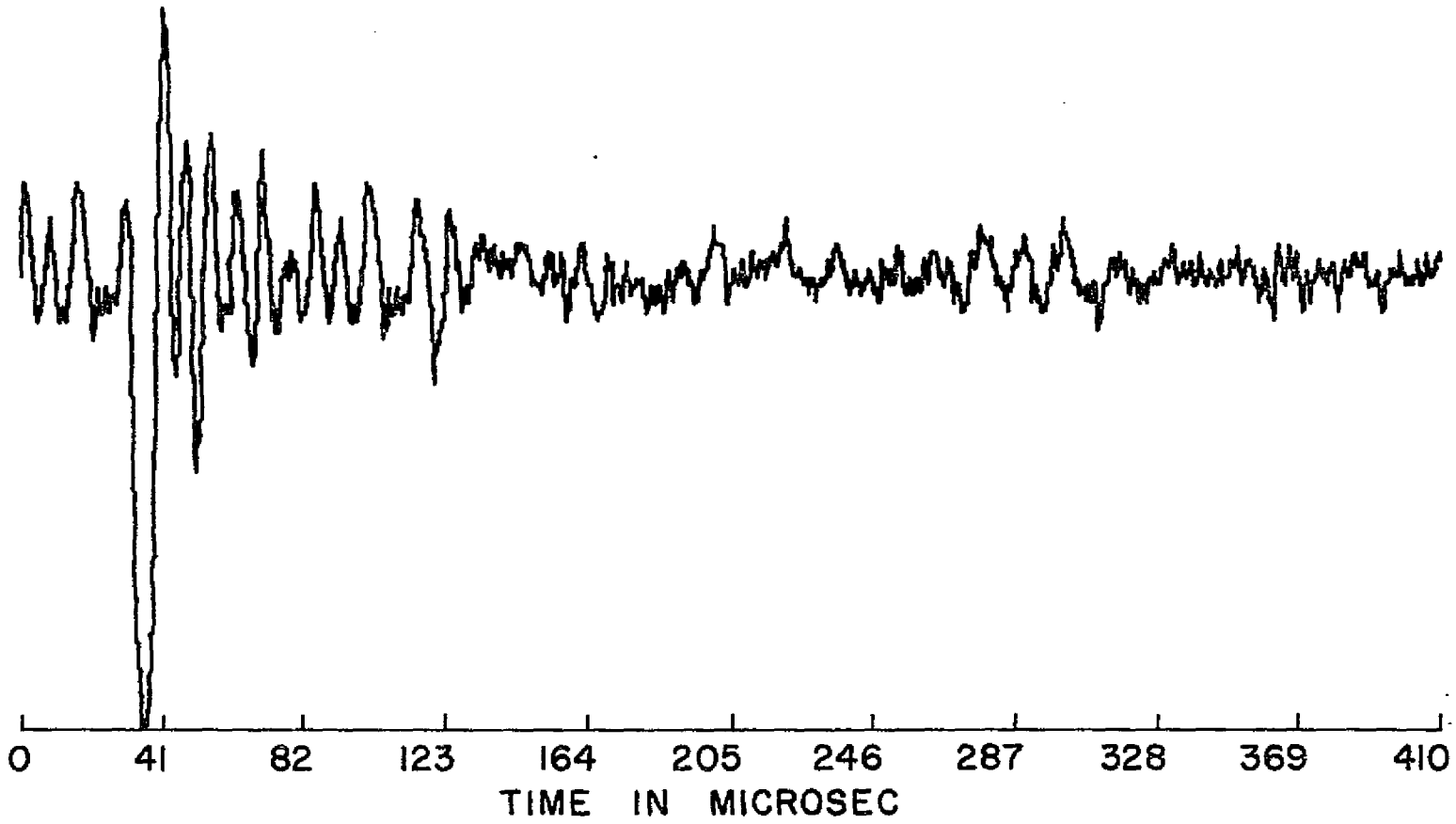

Figure 25. Acoustic Emission from the $[0/\pm45/90]_s$ Specimen at 2075 lbs. Load, Recorded by B & K Microphone, Normalized with Respect to the Maximum Amplitude

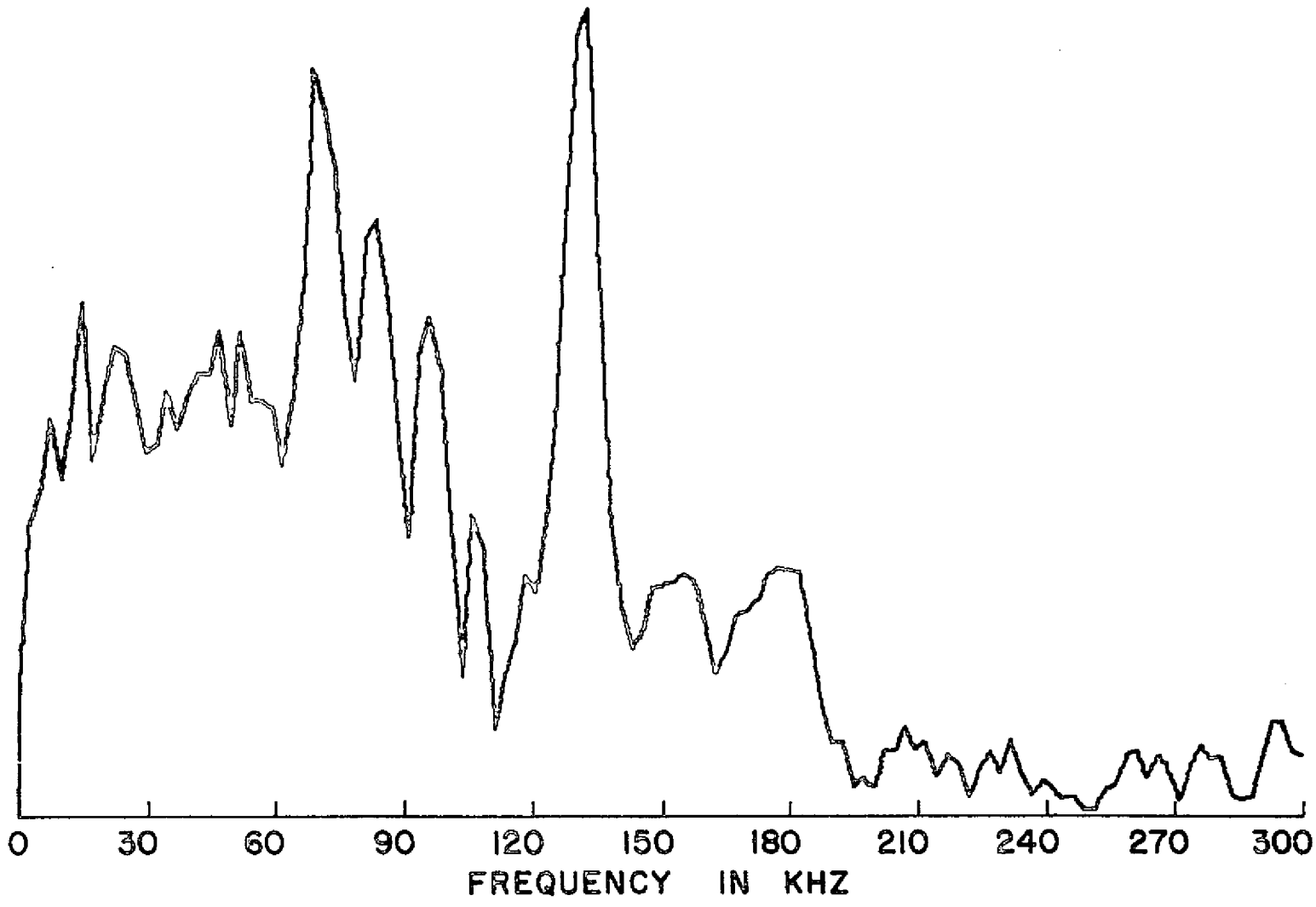

Fig. 26 Fourier Transform of Acoustic Emission Shown in Figure 25, Recorded by B & K Microphone from the $[0/\pm45/90]_s$ Specimen at 2075 lbs. Load

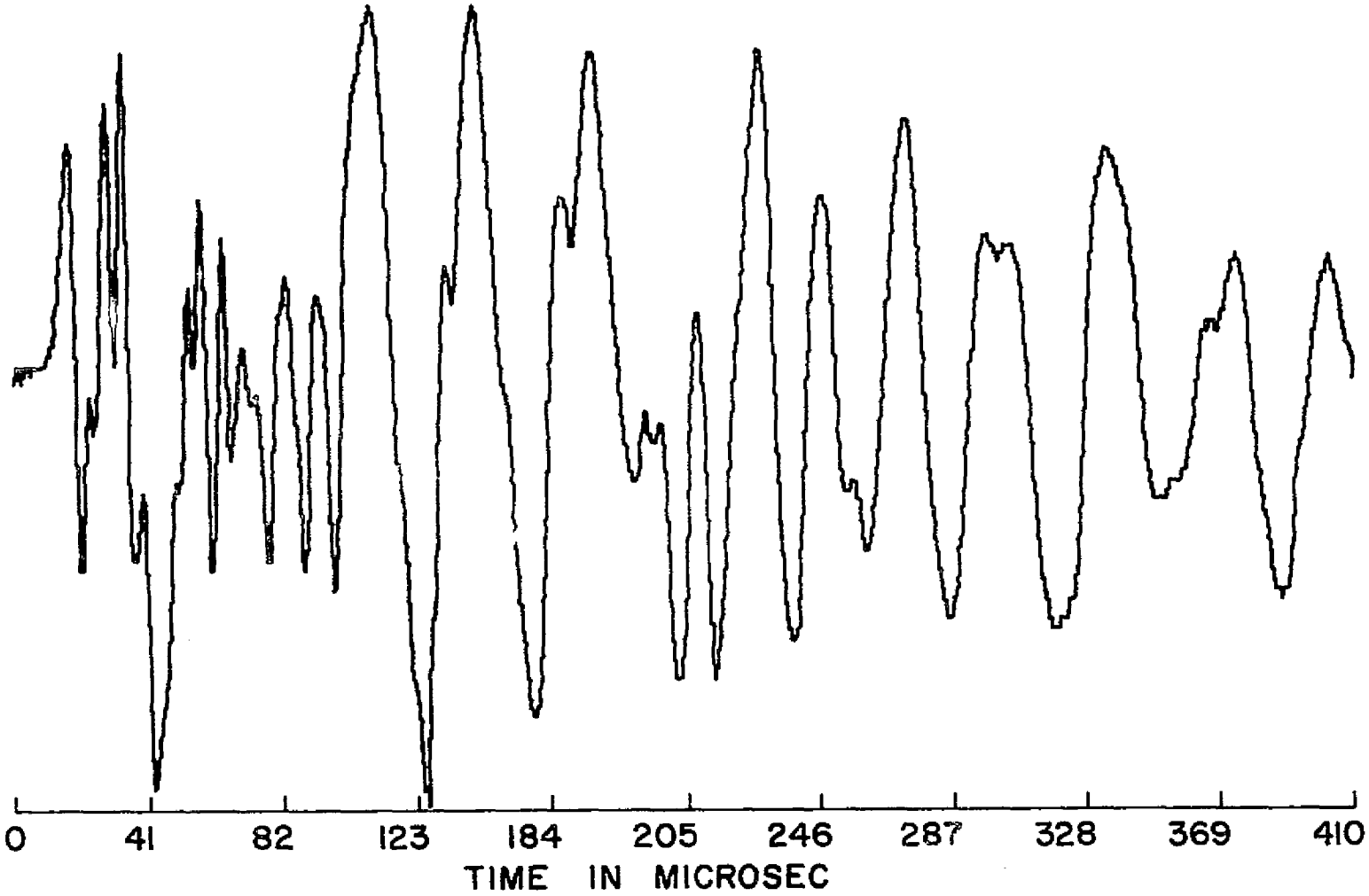

Fig. 27 Acoustic Emission from the $[0/\pm45/90]_s$ Specimen at 2500 lbs. Load, Recorded by the Transducer, Normalized with Respect to the Maximum Amplitude

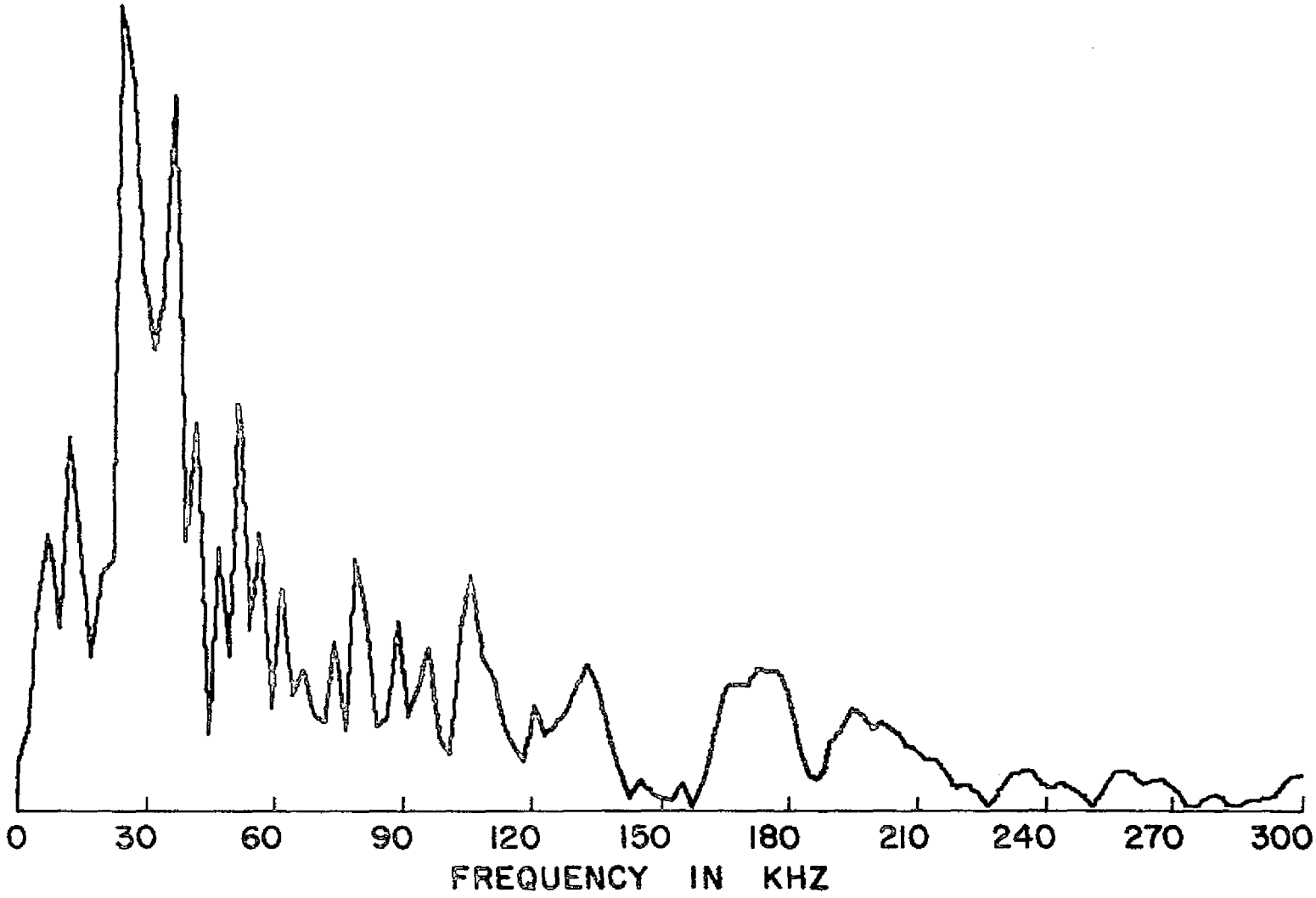

Fig. 28 Fourier Transform of Acoustic Emission Shown in Figure 27, Recorded by Transducer from the $[0/\pm45/90]_s$ Specimen at 2500 lbs. Load

best determined using the microphone. However, all other matrix cracking characteristics observable through the use of the transducer are present in both these emissions.

Figures 23 and 24 are an emission and its frequency transform recorded through the transducer at 1600 lbs. load at a voltage output from the tape recorder of .45 volts. Failure from 1600 lbs. up to 2100 lbs. is characterized by delaminations forming and growing between the 90°-90° interface and the 90°-45° interfaces [22]. The television camera verified that this type of behavior was occurring. This emission begins in a fashion similar to a fiber breakage type emission in that the amplitude of the first peak is smaller than the maximum and it rises to the maximum peak about 20 μsec. later. However, this emission decays very rapidly. Figure 25 and 26 are of an emission recorded with the microphone at a load level of 2075 lbs. Notice the rapid decline in the amplitude within the first 100 μsec. of the acoustic emission. The frequency transform, Figure 26, reveals an extremely broad frequency band, with large peaks up to 180 KHZ.

Figures 27 and 28 are of an emission recorded at 2500 lbs. load through the transducer. This emission appears to be two emissions rather than a single emission. The first emission seems to fit the model given as a fiber break in that it rises slowly to its maximum amplitude, but the decay is rapid as if it is a matrix crack type emission. The second emission follows a pattern like that of a fiber break type emission. The maximum amplitude of this emission at the tape recorder output was 3.8 volts.

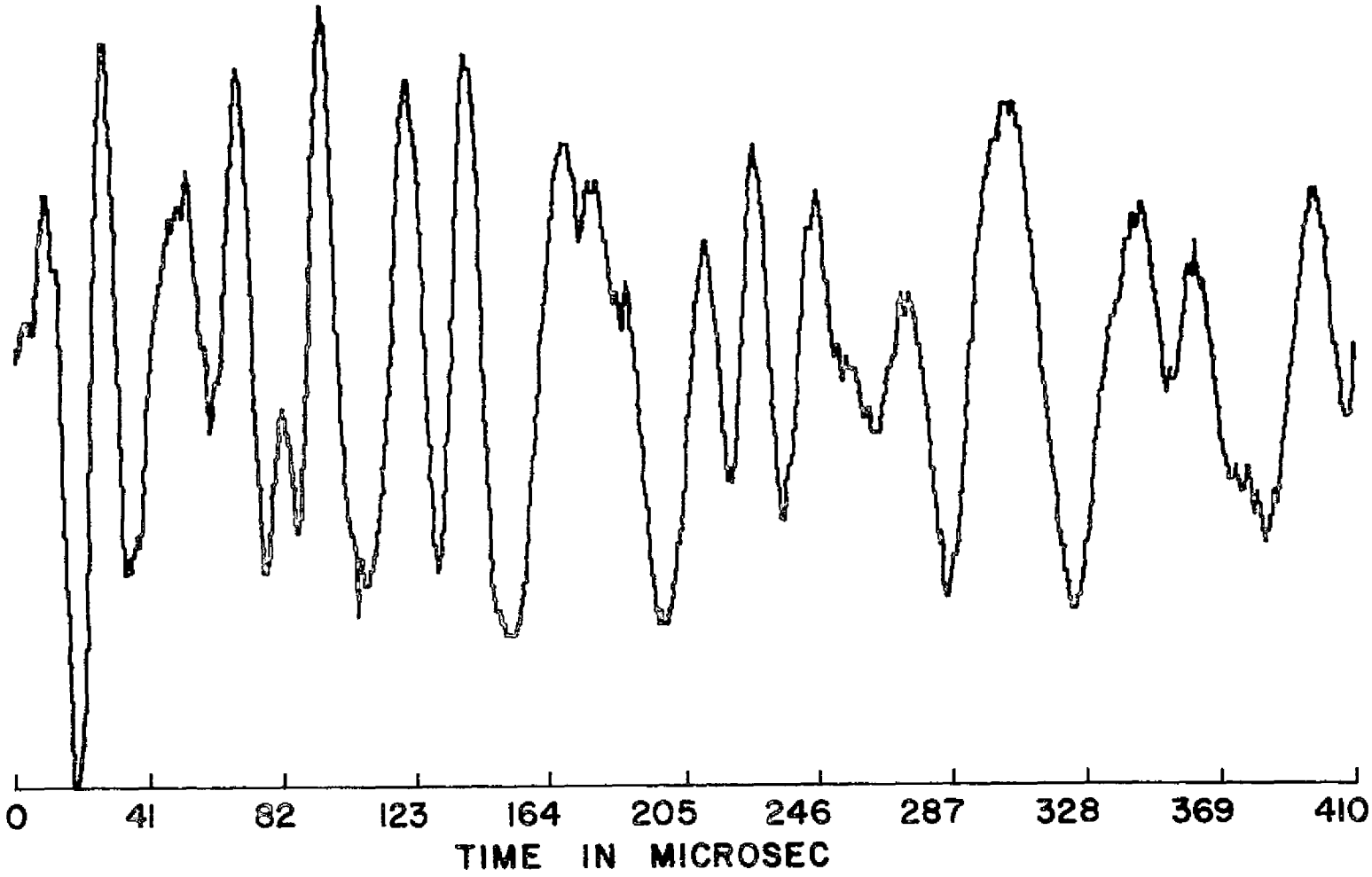

Figure 29. Acoustic Emission from the $[0/\pm45/90]_s$ Specimen at 3100 lbs. Load, Recorded by Transducer, Normalized with Respect to the Maximum Amplitude

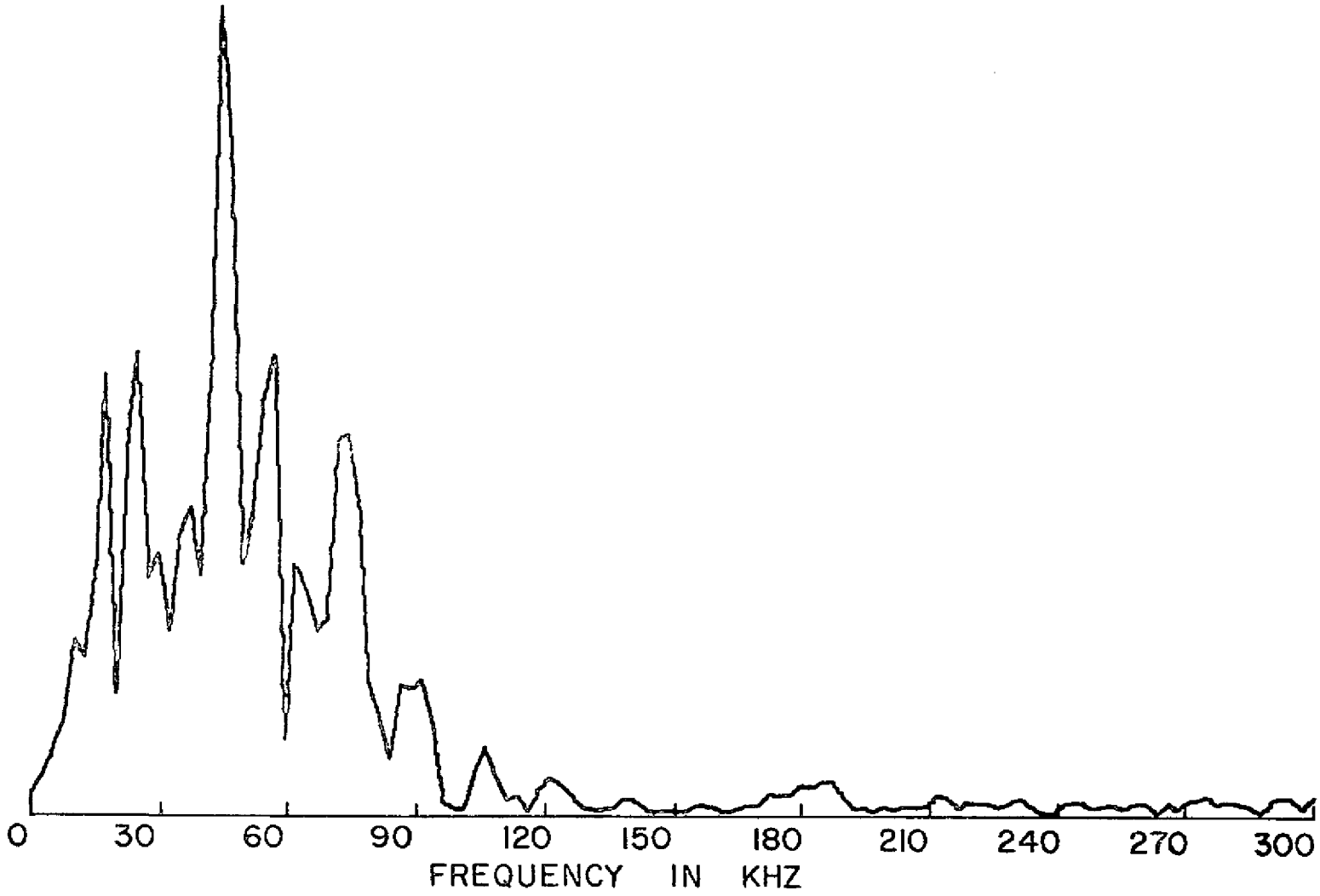

Figure 30. Fourier Transform of Acoustic Emission Shown in Figure 29, Recorded by Transducer from the $[0/\pm45/90]_s$ Specimen at 3100 lbs. Load

The acoustic emission shown in Figure 29 and its fourier transform, Figure 30 were recorded through the transducer at a load of 3100 lbs, just prior to specimen failure. The amplitude of this emission at the tape recorder output was .67 volts. The general shape of this emission fits the model appearance for an emission from a fiber failure. However, the amplitude was relatively low. The frequency content can not be compared with the model since this emission was only captured through the transducer.

5. CONCLUSIONS

In studying acoustic emissions consideration should be given to the mechanical and electrical vibration characteristics of the equipment and specimen. In generalizing the characteristics of a particular failure mode in the time domain the emission recorded through the FAC 500 transducer seems to offer the most obvious patterns. The emission recorded with the transducer may offer an envelope shape unique to a particular failure. The same emission seen in the time domain detected by the B and K microphone may lack discernable character. The additional high frequency components apparently hide some of the character of an emission in the time domain. However, any comparison of acoustic emissions in the fourier transformed domain should be of emissions recorded through use of a broad flat response detector such as the B and K microphone. Emissions recorded by the transducer have their frequency content distorted.

Because of the dominance of specimen mechnical resonances, only by comparing the frequency representations of two emissions from different failure processes from the same specimen can any trends be noted. The apparent difference in the frequency content of emissions from fiber breakage and matrix cracking is that the emissions from fiber breakage have a larger portion of their energy in higher frequencies. The emissions from matrix cracking contain energy primarily in frequencies below 120 KHZ. A large portion of the energy of emissions from fiber failure is contained in frequencies between 120 to 180 KHZ.

The most notable pattern for differentiating the type of failure source for an acoustic emission is found in the envelope in the time domain signal monitored by the transducer. Emissions from matrix cracking start by immediately rising to the peak amplitude and decaying almost completely in a 400 μsec. time frame. The envelope of emissions generated by a fiber break rise relatively slowly to a peak amplitude and decay slowly. Usually these emissions decay only slightly in a 400 μsec. time frame. The amplitude of fiber breakage type emissions is usually more than the amplitude of most emissions from a matrix cracking process. The exceptions to this rule seem to be emissions from a matrix crack that runs for a long distance.

The above trends were observed in single and unidirectional $[0_3]$ specimens. It was hoped that these trends could be found in more complicated laminates. However, the problem becomes more difficult when angle ply laminates are tested. Failure in engineering laminates occurs in many locations and makes correlation of an emission to a particular failure mode more difficult. Frequently, in engineering laminates several acoustic emissions will be generated almost simultaneously. Emissions occurring within the interior of a laminate are more constrained than those occurring in plies on the outside of a laminate or single ply laminates. The emissions occurring within a laminate would be expected to be of higher frequency because of the additional constraints imposed by surrounding material.

The single $[0/\pm45/90]_s$ specimen test provided a means of comparison of the model characteristics of failure in a unidirectional specimen

signal to acoustic emissions in an engineering laminate. Figures 19, 21, 23, and 25 were emissions that probably were generated by transverse cracking in matrix material or a delamination. All of these emissions have a character that suggested a matrix failure source. That is, these emissions raise to a peak amplitude rapidly and decay to the noise level rapidly.

The fiber break model can not be properly evaluated in real engineering laminates until a reliable method of detecting a single fiber failure event is devised. The study on the $[0/\pm45/90]_s$ specimens dealt with a replica study of the edges of the laminate [22]. The replica technique is only useful for surface damage processes. However, it would seem reasonable to expect a large portion of the acoustic emissions at loads approaching ultimate to be generated from fiber failure. Figures 27 and 29 are two emissions in the time domain at high load that seem to fit the model of a fiber failure type emission. Both of these emissions were detected by the transducer only. No acoustic emission in this test had large portions of its energy in the high frequencies as seen in the unidirectional laminate as an indication of fiber breakage. The frequency content of these emissions could have been changed by the additional constraints of the laminate configuration such that the higher frequencies were beyond the bandwidth of the equipment. If this happened the signal heard by the transducer would not necessarily be changed drastically since it could not detect the higher frequencies previously, but only shows an envelope composed of low frequencies which may not be altered.

The acoustic emissions shown from the $[0/\pm45/90]_s$ specimen are only a few of the emissions generated by this specimen. They are not intended as a complete group of emissions, or even typical ones, that occurred during this test. The time and cost of obtaining these few prevented a complete study of the acoustic emissions recorded during this test. The present method of analysis is too slow and requires too much shifting of the data from place to place. For a more complete study of acoustic emissions from an engineering laminate, such as the $[0/\pm45/90]_s$ specimen, a real time device should be used. More work should be done with various laminates to see if the observations of this study hold for various ply arrangements and for materials other than graphite-epoxy.

A study should be conducted to determine which wave types; i.e. Lamb, Rayleigh, dilational, shear or other; act as the means of transmission of an acoustic wave caused by an emission. This could be accomplished by using several transducers with various polarizations. All the transducers used in this study were polarized normal to the face that is, they measured the displacement normal to the surface on which they were mounted. It may be that certain types of failure result in a certain type of wave. This seems reasonable since the different modes of fracture cause different displacement fields and relieve different stress states.

A transfer function should be obtained for the FAC 500 transducer. By using a transfer function it would be possible to correct the poor response characteristics of the transducer. Although the B and K

microphone has good response characteristics it has poor sensitivity. Also background noise is picked up by the microphone. The transducer is very sensitive and does not pick up the background noise. Most techniques such as reciprocity calibration [19] require a knowledge of the type of wave being propagated. This makes determining the mode of propagation for acoustic emissions in the specimens very important.

REFERENCES

1. Henneke, E. G., II, Herakovich, C. T., Jones, G. L. and Renieri, M. P., "Acoustic Emission from Composite-Reinforced Metals," Experimental Mechanics, Vol. 15, No. 1, pp. 10-16, 1975.

2. Harris, D. O. and Bell, R. L., "The Measurement and Significance of Energy in Acoustic Emission Testing," Tech Rep. DE-74-3A, Dunegan/Endevco, San Juan Capistrano, Ca. (Jan. 1974).

3. Rothwell, R. and Arrington, M., "Acoustic Emission and Micromechnical Debond Testing," Nature Physical Science, Vol. 233, Oct. 1971, pp. 163-164.

4. Dunegan, H. L., "Listening ... the Liberty Bell," Dunegan/Endevco, San Juan Capistrano, Ca. (Aug. 1976).

5. Curtis, G., "Acoustic Emission - 4, Spectral Analysis of Acoustic Emission," Non-Destructive Testing, April 1974, pp. 82-91.

6. Graham, L. J. and Alers, G. A., "Detection and Analysis of Fracture with Acoustic Emission," Preprint no. 72-99, North American Rockwell Science Center.

7. Graham, L. J. and Alers, G. A., "Frequency Spectra of Acoustic Emissions Generated by Deforming Metals and Ceramics," IEEE, Ultrason. Symp. Proc., 1972, pp. 18-21.

8. Fleischmann, P., Rouby, D., Lakestani, F. and Baboux, J. C., "A Spectral Analysis of Acoustic Emisssion," Non-Destructive Testing, Oct. 1975, pp. 241-244.

9. Ono, K. and Ucisik, H., "Acoustic Emission Behavior of Aluminum Alloys," Materials Evaluation, Vol. 34, Feb. 1976, pp. 32-44.

10. Beattie, A. G., "Characteristics of Acoustic Emission Signals Generated by a Phase Transition," IEEE Proceedings, 1972, pp. 13-17.

11. Speake, J. H. and Curtis, G. J., "Characterization of the Fracture Processes in CFRP Using Spectral Analysis of Acoustic Emissions Arising from the Application of Stress," International Conference on Carbon Fibers, their Place in Modern Technology, London, Feb. 1974, Paper No. 29.

12. Mehan, R. L. and Sturgeon, L., "Spectral Analysis of Acoustic Events Observed in B/Al and B/Epoxy," Private Communication.

13. Mullin, J. V. and Mehan, R. L., "Evaluation of Composite Failures

through Fracture Signal Analysis," Journal of Testing and Evaluation, JTEVA, Vol 1, No. 3, May 1973, pp. 215-219.

14. Henneke, E. G., II, and Herring, H. W., "Spectral Analysis of Acoustic Emissions from Boron-Aluminum Composites," Composite Reliability, ASTM STP 580, American Scoeity for Testing and Materials, 1950, pp. 202-214.

15. Meirovitch, L., Analytic Methods in Vibrations, The MacMillan Company, New York, New York, 1967.

16. Meirovitch, L., Elements of Vibration Analysis, McGraw-Hill, New York, New York, 1975.

17. Brigham, E. O., The Fast Fourier Transform, Prentice-Hall, Inc., Englewood Cliffs, New Jersey, 1974.

18. Coley, J. W., Lewis, P. A. W. and Welch, P. D., "The Fast Fourier Transform and Its Applications," IEEE Transactions on Education, Vol. 12, 1969, No. 1, pp. 27-34.

19. Wilson, G. H., III, "A Microprocessor-Based System for Laboratory Data Acquisition," Virginia Polytechnic Institute and State University, Masters Thesis (1975).

20. O'Brien, D. A.,,"Modified Procedure for Interfacing Between Biomation 805 and CB^2 System," Intradepartment Memo.

21. Hatano, H. and Mori, E., "Acoustic Emission Transducer and Its Absolute Calibration," Journal of the Acoustical Society of America, Vol. 59, No. 2, Feb. 1976, pp. 344-349.

22. Stalnaker, D. O., "An Investigation of Edge Damage Development in Quasi-Isotropic Graphite/Epoxy Laminates," Virginia Polytechnic Institute and State University, Masters Thesis (1977).

23. Newland, D. E., An Introduction to Random Vibrations and Spectural Analysis, Longman Group Limited, London, 1975.

APPENDIX

PROGRAM FOR ACOUSTIC EMISSION ANALYSIS

The program performs the fast fourier transform on a digital series representation of a signal. The plot output consists of plots of the signal and its fourier transform. The print out contains the mean, maximum, and minimum of the signal and the amplitude and frequency of the peaks of the fourier transform.

Input of the signal is 2048 data points in a 10(5X, F3.0) format. The program will analyze data that is digitized either .2, .5 or 1.0 μ secs./pt. The value of NBIOST controls this feature. NBIOST should be 10^7 times the digitization interval in seconds.

If other than 2048 data points compose the input signal, some alteration is required. The number of points should always allow the following equation to be satisfied.

$$NB = 2^N$$

Where N is an integer and NB is the number of points that compose the signal being analyzed. If other than 2048 points are used the values of N and NB must be changed as well as the array sizes in the dimension statement in the main program. Additional zeros may be added to the signal to satisfy the above equation. If the length of time of the signal is other than 409.4, 1023.5 or 2047 μs. the second CALL SAXIS card must be changed to account for the different length of time on the plot outputs. If the digitization interval is different from .2, .5 or

1.0 μs./pt. the first CALL SAXIS must be changed to provide for the different frequency scale on the frequency plot.

SUBROUTINE FFT outputs to the main program a series of complex numbers that form the fourier transform of the input series. The main program plots the amplitude of the fourier transform only. A complete discussion of this subroutine is contained in reference 23.

```
C   $$$$$$$$$$$$$$$$$$$$$$$$$$$$$$$$$$$$$$$$$$$$$$$$$
C   $$$$  ACOUSTIC EMISSION FOURIER ANALYSIS  $$$$
C   $$$$  SAMUEL S. RUSSELL                   $$$$
C   $$$$$$$$$$$$$$$$$$$$$$$$$$$$$$$$$$$$$$$$$$$$$$$$$
      DIMENSION B(2048),SKALE(2048),AMAG(1024)
      COMPLEX A(2048),CMPLX
C ****************************************************************
C   PARAMETER LIST
      NBIOST=2
C   NBIOST IS TIME DISCRETIZATION PARAMETER
C   NBIOST=2 --- .2 MICROSECONDS PER POINT
C   NBIOST=5 --- .5 MICROSECONDS PER POINT
C   NBIOST=10 --- 1 MICROSECONDS PER POINT
      NB=2048
C   NB IS NUMBER OF POINTS THAT COMPOSE SIGNAL TO BE ANALYZED
      N=11
C   N COMPUTED SUCH THAT NB=2**N
      NBACK=0
C   IF SIGNAL IS BACKWARD NBACK=1
      SIZEX1=8.0
C ****************************************************************
C   INITIALIZE
      AMAX=0.0
      BMAX=0.0
      BMIN=0.0
      SUM=0.0
      NBO2=NB/2
  100 FORMAT(10(5X,F3.0))
  101 FORMAT(3X,'B=',E11.4,3X,'I=',I5)
  102 FORMAT(3X,'MAX SIGNAL INPUT ',E11.4,3X,'MIN SIGNAL INPUT ',E11.4,/
     1/,3X,'MAX FREQUENCY COMPONENT ',E11.4)
  103 FORMAT(3X,'AVE. INPUT=',E11.4)
```

```
      READ(5,100)(B(I),I=1,NB)
      DO 1 I=1,NB
      IF(B(I).GT.BMAX)BMAX=B(I)
      IF(B(I).LT.BMIN)BMIN=B(I)
      SUM=SUM+B(I)
    1 CONTINUE
      AVE=SUM/NB
C     WRITE MEAN OF SIGNAL
      WRITE(6,103)AVE
      IF(NBACK.NE.1)GO TO 23
      DO 21 I=1,NB02
      TEMP=B(I)
      B(I)=B(NB+1-I)
   21 B(NB+1-I)=TEMP
      DO 24 I=1,40
      WRITE(6,101)B(I),I
   24 IF(B(I).EQ.0.0)B(I)=AVE
      GO TO 25
   23 CONTINUE
      DO 26 I=1,40
      J=NB-40+I
      WRITE(6,101)B(J),J
   26 IF(B(J).EQ.0.0)B(J)=AVE
   25 CONTINUE
C     CREATE DISPLACED COSINE WINDOW
      DO 3 I=1,NB
      THETA=3.14159265*(I-1)/2047.0
    3 SKALE(I)=1.0/2.0+COS(THETA)/2.0
    4 DO 2 I=1,NB
      B(I)=B(I)-AVE
      A(I)=CMPLX(B(I),0.0)*SKALE(I)
    2 CONTINUE
```

```
C  PERFORM THE FOURIER TRANSFORM
      CALL FFT(A,N,NB)
      CALL SCALE(B,NB,2.5)
      DO 5 I=1,NB02
      AMAG(I)=CABS(A(I))
      IF(AMAG(I).GT.AMAX)AMAX=AMAG(I)
    5 CONTINUE
      CALL SCALE(AMAG,NB02,5.0)
      WRITE(6,102)BMAX,BMIN,AMAX
      BMAX=0.0
      DO 22 I=1,NB
   22 IF(B(I).GT.BMAX)BMAX=B(I)
      WRITE(6,102)BMAX
      CALL PLOT(4.0,3.5,-3)
      CALL PLT2(NB02,AMAG,SIZEX1,B,NB,AMAX,NBIOST)
      CALL PLOT(0.0,0.0,-4)
      STOP
      END
```

```
C SUBROUTINE PLT2 PLOTS SIGNAL, FOURIER TRANSFORMS SIGNAL, AND PRINTS
C  AMPLITUDE AND FREQUENCY OF PEAKS IN THE FOURIER TRANSFORMED SIGNAL
      SUBROUTINE PLT2(NBO2,AMAG,SIZEX,B,NB,AMAX,NBIOST)
      DIMENSION AMAG(NBO2),B(NB),LABLE1(10),LABLE2(10)
      DATA LABLE1/'FREQ','UENC','Y IN',' KHZ',6*'    '/,LABLE2/'TIME','
     1IN ','MICR','OSEC',6*'    '/
      N=0
      NBM3=NBO2-3
      DO 3 I=3,NBM3
      AM=AMAG(I)*AMAX/5.0
      SAMX=AMAG(I)*2.0-AMAG(I-2)-AMAG(I-1)
      SANN=AMAG(I)*2.0-AMAG(I+2)-AMAG(I+1)
      FREQ=(I-1)/(NBIOST*2.0E-07*(NBO2-1))
  100 FORMAT(3X,'MAG=',E12.5,3X,'FREQ=',F12.5,'HZ')
    3 IF((SAMX.GE.0.0).AND.(SANN.GE.0.0).AND.(AMAG(I).GE.1.0))WRITE(6,10
     10)AM,FREQ
      NBTP3=NB*3/100*NBIOST+1
      DO 9 I=1,NBTP3
      DX=(I-1)*SIZEX/(NBTP3-1)
    9 CALL PLOT(DX,AMAG(I),2)
      CALL PLOT(0.3,0.0,3)
      CALL SAXIS(0.0, 0.0,LABLE1,-16, 9.1,0.0,0.0,30.00,0.80,0.0)
      CALL PLOT(SIZEX+3.0,2.5,-3)
      DO 7 I=1,NB
      DX=(I-1)*SIZEX/(NB-1)
    7 CALL PLOT(DX,B(I),2)
      CALL PLOT(0.0,0.0,3)
      IF(NBIOST.EQ.2)CALL SAXIS(0.0,-2.5,LABLE2,-16,6.1,0.0,0.0,40.96,0.
     180,0.0)
      IF(NBIOST.EQ.5)CALL SAXIS(0.0,-2.5,LABLE2,-16,8.1,0.0,0.0,102.35,0
     1.80,0.0)
      IF(NBIOST.EQ.10)CALL SAXIS(0.0,-2.5,LABLE2,-16,8.1,0.0,0.0,204.70,
```

```
10.30,0.0)
 CALL PLOT(SIZEX,0.0,-3)
 RETURN
 END
```

```
C  SUBROUTINE FFT PERFORMS FAST FOURIER TRANSFORM
      SUBROUTINE FFT(A,N,NB)
      COMPLEX A(NB),U,W,T
      DO 1 J=1,NB
    1 A(J)=A(J)/NB
      NBD2=NB/2
      NBM1=NB-1
      J=1
      DO 4 L=1,NBM1
      IF(L.GE.J)GO TO 2
      T=A(J)
      A(J)=A(L)
      A(L)=T
    2 K=NBD2
    3 IF(K.GE.J)GO TO 4
      J=J-K
      K=K/2
      GO TO 3
    4 J=J+K
      PI=3.1415926535897#3
      DO 6 M=1,N
      U=(1.0,0.0)
      ME=2**M
      K=ME/2
      W=CMPLX(COS(PI/K),-SIN(PI/K))
      DO 6 J=1,K
      DO 5 L=J,NB,ME
      LPK=L+K
      T=A(LPK)*U
      A(LPK)=A(L)-T
    5 A(L)=A(L)+T
    6 U=U*W
```

RETURN
END

```
C  SUBROUTINE SCALE -- SCALES A SERIES OF DATA POINTS
C  X=== SERIES BEING SCALED, N== NUMBER IN SERIES, HT== AMPLITUDE TO
C  SCALE TO
      SUBROUTINE SCALE(X,N,HT)
      DIMENSION X(N)
      XMAX=X(1)
      DO 10 I=1,N
      A=ABS(X(I))
   10 XMAX=AMAX1(XMAX,A)
      SF=HT/XMAX
      DO 20 I=1,N
   20 X(I)=X(I)*SF
      RETURN
      END
```